Bachelor-Thesis: Truncated Lieb-Liniger model with quasi-spin 1/2

Simon Bachhuber, Matrikelnummer: 1768044

Submitted in June 2018

UNIVERSITY REGENSBURG
Physics faculty

Supervised by Prof. Dr. Klaus Richter

Contents

1. Introduction

Solving Many-particle systems is a highly complicated task in quantum mechanics. Exactly solving the Schrödinger equation of one atom of an element of the periodic table is only possible for hydrogen. The next "simplest" element, Helium, consisting of only two electrons, protons and neutrons, is already unsolved.
Therefore, approximations are needed. One example is Mean-field-theory, where one approximates an interacting Many-particle system as a system of free particles in an external field.
Another example is to reduce the system's, often indefinitely large, phase space to a phase space of finite size by some form of truncation.
Obviously, this cutoff comes at the cost of unconsidered phase space but it still might reveal properties or tendencies of the actual system.
In this thesis the model of interest is the Lieb-Liniger model and a (strongly) modified version of it.
The Lieb-Liniger model is an example of a quantum integrable model, a model that is solvable with the Bethe Ansatz, and one can, using the Yang-Baster relation, get the "transfer matrix" to then generate an infinite set of conserved quantities[7].
It was introduced in 1963, roughly 40 years after the birth of quantum mechanics, by Elliott H. Lieb and Werner Liniger.
Despite its simplicity, it is a fascinating Many-body system of a one-dimensional gas of Bose particles interacting via a repulsive delta-function potential[6].
In the same paper Lieb and Liniger solved this quantum integrable model using the Bethe ansatz.
For this matter, the Bethe ansatz was invented 1931 by Hans Bethe in order to find the exact eigenvalues of the one-dimensionial antiferromagnetic Heisenberg model.
The model gained popularity for one crucial reason. It was the only exactly solvable model with a "realistic" two-body potential, a potential that actually exists in a gas, apart of Girardeau's model. Girardeau showed that a gas of impenetrable bosons has the same energy spectrum as a gas of noninteracting fermions[6].
In this thesis we first look at a momentum-truncated version of the Lieb-Liniger model with parabolic dispersion relation and then replace the parabolic- by a linear dispersion relation. A necessary tool for this task is second quantization, hence the first chapter is a very brief overview of it.
The major part of the thesis is about a truncated Lieb-Liniger model with linear dispersion relation and quasi-spin 1/2.
This is a possible approximation of a bosonic gas with a two-band structure in the environment of a crossing in the system's dispersion relation.
In any case the strategy is to first establish an enumerated list of all the allowed states of the system, then to display the Hamiltonian as a matrix using latter list as a basis and then diagonalize it.
Only the calculation of the Hamiltonian in second quantization is done analytically, the remaining work is of numerical nature and performed with Wolfram Mathematica.

2. General concepts

2.1. Most general N-particle Hamiltonian with two-particle interaction

Let's assume we have a Hamiltonian given by

$$H = H_0 + V = \sum_{\alpha=1}^{N} t_\alpha + \sum_{\alpha<\beta} V_{\alpha\beta} \tag{1}$$

where α and β label the individual particles.
We take a look at the single-particle part of the Hamiltonian first. We can rewrite

$$\begin{aligned} H_0 &= \sum_\alpha \sum_i |i\rangle_\alpha \langle i|_\alpha \, t_\alpha \sum_j |j\rangle_\alpha \langle j|_\alpha \\ &= \sum_{i,j} \langle i|t|j\rangle \, a_i^\dagger a_j \\ &= \sum_{i,j} t_{ij} a_i^\dagger a_j, \end{aligned}$$

using the known relation for completeness if the chosen basis is complete and orthonormal

$$\sum_i |i\rangle \langle i| = 1$$

and also the important equation

$$\sum_{\alpha=1}^{N} |i\rangle_\alpha \langle j|_\alpha = a_i^\dagger a_j$$

valid for arbitrary N and only in the symmetric Hilbertspace of bosons. In the latter equation $a_i^\dagger$ and a_i are the creation- and annihilation-operators

$$a_i^\dagger |\Omega\rangle = |i\rangle_\alpha \,, \; a_i |i\rangle_\alpha = |\Omega\rangle \,, \; a_i |\Omega\rangle = 0.$$

Here $|\Omega\rangle$ is the zero-particle-state ket. They satisfy the (commutator) relations

$$n_k \equiv a_k^\dagger a_k, \qquad [a_k, a_{k'}^\dagger] = \delta_{k,k'}, \qquad [a_k, a_{k'}] = [a_k^\dagger, a_{k'}^\dagger] = 0. \tag{2}$$

For a proof see, e.g., [1]. In the same fashion one can show that for the two-particle-interaction part of the Hamiltonian you may write

$$\begin{aligned} V &= \frac{1}{2} \sum_{i,j,k,m} \langle i,j|V|k,m\rangle \, a_i^\dagger a_j^\dagger a_m a_k \\ &= \frac{1}{2} \sum_{i,j,k,m} V_{ijkm} a_i^\dagger a_j^\dagger a_m a_k. \end{aligned}$$

Thus, the entire Hamiltonian of a N-particle system with two-particle interaction in second quantization is given by

$$H = \sum_{i,j} t_{ij} a_i^\dagger a_j + \frac{1}{2} \sum_{i,j,k,m} V_{ijkm} a_i^\dagger a_j^\dagger a_m a_k. \tag{3}$$

2.2. Lieb-Liniger model

We discuss moving particles in one dimension with periodic boundary conditions, i.e., on a ring of length R. Furthermore there is a very short-ranged coupling, modeled by a contact potential, allowing them to bounce off of each other or being attracted and thus stick to each other. Strictly speaking, only the repulsive case is the Lieb-Liniger model. The Lieb-Liniger model is interesting since a quantum phase transition might occur.
Quantum phase transition describes a phase transition between different quantum phases at zero temperature. It describes a sudden change of the ground state wave function of a Many-body system[8].
Quantum phase transitions occur in the limit $N \to \infty$ but some indications are observable at finite particle numbers. For instance, a sudden change or discontinuity in the first or higher derivatives of the energy as a function of an external parameter, in our case the strength of the coupling, can indicate a quantum phase transition[9].
Another example is the vanishing of the Bogoliubov excitation energy, i.e., at the phase transition the Bogoliubov approximation is never valid and breaks down[10]. A visible effect of this phenomena is a narrowing spectrum and an energy collapse on the ground state energy.
The point, in the coupling constant, at which the quantum phase transition most likely occurs, due to the indicator's implication, is from now on referred to as the critical point.
The Hamiltonian of the Lieb-Liniger model with N particles in first quantization is of the form

$$H = -\frac{\hbar^2}{2m}\sum_{\alpha=1}^{N}\frac{\partial^2}{\partial x_\alpha^2} - 2R\alpha \sum_{\alpha\neq\beta,\alpha<\beta}\delta(x_\alpha - x_\beta) = H_0 - \alpha V.$$

Going into second quantization using plane waves as a basis,

$$\begin{aligned}\langle x|\psi_k\rangle &= \psi_k(x) = \frac{1}{\sqrt{R}}e^{i\frac{2\pi}{R}kx}, \quad k \in \mathbb{Z}\\ \langle k|k'\rangle &= \int dx \psi_k^*(x)\psi_{k'}(x) = \delta_{k,k'}, \quad \forall k,k' \in \mathbb{Z}\end{aligned} \tag{4}$$

with the Kronecker delta defined as

$$\delta_{k,k'} = \begin{cases}1 & k = k'\\ 0 & \text{else}\end{cases},$$

we then must calculate

$$t_{kk'} = \langle k|t|k'\rangle = \frac{-\hbar^2}{2m}\frac{1}{R}\int dx e^{-i\frac{2\pi}{R}kx}\frac{\partial^2}{\partial x^2}e^{i\frac{2\pi}{R}k'x} = \frac{\hbar^2}{2m}\left(\frac{2\pi k'}{R}\right)^2\delta_{k,k'},$$

$$\begin{aligned} v_{klmn} &= \langle k,l|V(x,x')|n,m\rangle \\ &= \frac{-2R\alpha}{R^2}\int\int dxdx' e^{-i\frac{2\pi}{R}kx}e^{-i\frac{2\pi}{R}lx'}\delta(x-x')e^{i\frac{2\pi}{R}nx}e^{i\frac{2\pi}{R}mx'} \\ &= \frac{-2R\alpha}{R^2}\int dx e^{i\frac{2\pi}{R}x(n+m-k-l)} \\ &= -2\alpha\delta_{k+l,m+n}. \end{aligned}$$

Therefore the Hamiltonian in k-space is given by

$$H = \frac{-\hbar^2}{2m}\sum_{k,k'} -\left(\frac{2\pi k'}{R}\right)^2 \delta_{k,k'}a_k^\dagger a_{k'} - \frac{2R\alpha}{2R}\sum_{k,l,m,n}\delta_{k+l,m+n}a_k^\dagger a_l^\dagger a_m a_n \tag{5}$$

$$= \frac{\hbar^2}{2m}\left(\frac{2\pi}{R}\right)^2\sum_k k^2 a_k^\dagger a_k - \alpha\sum_{k,l,m,n}\delta_{k+l,m+n}a_k^\dagger a_l^\dagger a_m a_n. \tag{6}$$

2.3. Truncated Lieb-Liniger-Model

In general, in the Hamiltonian (6) we have to sum over all possible values for k, being all the integer numbers. This is too difficult of a task, hence we introduce a cut-off at a certain k-mode - the higher the k-mode the more accurate the approximation. The error increases when the system goes to high energies since the higher k-modes would have bigger significance.

3. Three-site-case and five-site-case for arbitrary total momentum L with spin zero

First, we briefly discuss the easiest case of the truncated Lieb-Liniger-Model, by only allowing for values of $\pm 1, 0$ for the k-mode of a single-particle. This is strictly following Benjamin Geiger's approach of the 3-site and 5-site model given in the Mathematica sheet[2].
This was mostly done to understand the numerical procedure and check, if the obtained results matched the ones from Benjamin. Another reason was to get familiar with quantum phase transitions since, for this model, it was already known to have a critical point.
We assume our particles to be bosonic of spin zero, so there is no spin degree of freedom

and set $R = 2\pi$ and $\frac{\hbar^2}{2m} = 1$. The Hamiltonian of the system then is

$$
\begin{aligned}
H &= \sum_{k=\pm1,0} k^2 a_k^\dagger a_k - \alpha \sum_{k,l,m,n=\pm1,0} \delta_{k+l,m+n} a_k^\dagger a_l^\dagger a_m a_n \qquad (7)\\
&= a_1^\dagger a_1 + a_{-1}^\dagger a_{-1} - \alpha\Big(\sum_{k=\pm1,0} a_k^\dagger a_k^\dagger a_k a_k + 4\big(n_1 n_0 + n_{-1} n_0 + n_1 n_{-1}\big) \\
&\qquad + 2(a_0^\dagger a_0^\dagger a_1 a_{-1} + a_1^\dagger a_{-1}^\dagger a_0 a_0)\Big) \\
&= a_1^\dagger a_1 + a_{-1}^\dagger a_{-1} - \alpha\Big(\sum_{k=\pm1,0} a_k^\dagger (a_k a_k^\dagger - 1) a_k + 4\big(n_1 n_0 + n_{-1} n_0 + n_1 n_{-1}\big) \\
&\qquad + 2(a_0^\dagger a_0^\dagger a_1 a_{-1} + (a_0^\dagger a_0^\dagger a_1 a_{-1})^\dagger)\Big) \\
&= n_1 + n_{-1} - \alpha\Big(\sum_{k=\pm1,0} (n_k^2 - n_k) + 4\big(n_1 n_0 + n_{-1} n_0 + n_1 n_{-1}\big) \\
&\qquad + 2(a_0^\dagger a_0^\dagger a_1 a_{-1} + (a_0^\dagger a_0^\dagger a_1 a_{-1})^\dagger)\Big) \\
&= h_0 - \alpha\big(h_{diag} + h_{offdiag} + h_{offdiag}^\dagger\big).
\end{aligned}
$$

For this derivation we used the definition of the occupation-number-operator and the bosonic commutator relation given in equation (2).
In order to diagonalize this Hamiltonian we need to choose a basis first

$$
|n_{-1}, n_0, n_1\rangle = |n_{-1} = n_1 - L, n_0 = N - 2n_1 + L, n_1\rangle \equiv |N, L, n\rangle\,. \qquad (8)
$$

We can see that a unique state was initially characterized by three occupation numbers, but it is reducible to just one due to the fact that we have two integrals of motion given by the number of particles N and the overall momentum L of the system

$$
\begin{aligned}
N &= n_1 + n_0 + n_{-1},\\
L &= \sum_{k=0,\pm1} k n_k = n_1 - n_{-1}. \qquad (9)
\end{aligned}
$$

Now, we may check the action of the Hamiltonian on our basis using the known relations

$$
a^\dagger |n\rangle = \sqrt{n+1}\,|n+1\rangle\,, \qquad\qquad a\,|n\rangle = n\,|n-1\rangle\,.
$$

Starting with the off diagonal term

$$
\begin{aligned}
a_0^\dagger a_0^\dagger a_1 a_{-1}\,|n\rangle &= \sqrt{n-L}\sqrt{n}\sqrt{N-2n+L+1}\sqrt{N-2n+L+2}\\
&\qquad |n_1 - L - 1, N - 2n_1 + L + 2, n_1 - 1\rangle\\
&= \sqrt{n-L}\sqrt{n}\sqrt{N-2n+L+1}\sqrt{N-2n+L+2}\,|n-1\rangle\,,
\end{aligned}
$$

we can already see that the three-site-case with no spin is especially easy since only the diagonal and first off-diagonal elements are unequal to zero. The whole Hamiltonian is then given by

$$\begin{aligned}
H_{nm} &= \langle n|H|m\rangle = \langle n|h_0|m\rangle - \alpha\Big(\langle n|h_{diag}|m\rangle + \langle n|h_{offdiag}|m\rangle + \langle n|h^\dagger_{offdiag}|m\rangle\Big) \\
&= \delta_{n,m}\Big(2m - L - \alpha\Big[m^2 - m + (N-2m+L)^2 - (N-2m+L) + (m-L)^2 \\
&\qquad - (m-L) + 4\big(m(N-2m+L) + (m-L)(N-2m+L) + m(m-L)\big)\Big]\Big) \\
&- \delta_{n,m-1}2\alpha\sqrt{m-L}\sqrt{m}\sqrt{N-2m+L+1}\sqrt{N-2m+L+2} \\
&- \big(\delta_{n,m-1}2\alpha\sqrt{m-L}\sqrt{m}\sqrt{N-2m+L+1}\sqrt{N-2m+L+2}\big)^T \\
&= \delta_{n,m}\Big(2m - L + \alpha\big[4mN - 6m^2 + (N-1)N\big]\Big) \\
&- \delta_{n,m-1}2\alpha\sqrt{m-L}\sqrt{m}\sqrt{N-2m+L+1}\sqrt{N-2m+L+2} \\
&- \delta_{m,n-1}2\alpha\sqrt{n-L}\sqrt{n}\sqrt{N-2n+L+1}\sqrt{N-2n+L+2}.
\end{aligned}$$

Without loss of generality the total momentum L is greater or equal to zero and its maximal value is - due to equation (9) - N. So, the last step is to figure out the range of the allowed states, i.e., the minimal and maximal values of the occupation number n_1 for a given N and L. This is simply

$$n_{1_{min}} = L, \qquad\qquad n_{1_{max}} = \lfloor\frac{N-L}{2}\rfloor + L. \tag{10}$$

Therefore, our Hamiltonian is of the dimension $\lfloor\frac{N-L}{2}\rfloor + 1$ and also has the same number of eigenvalues.

Figure (1) is a plot of the energy difference of the exited states and the groundstate as a function of the combined parameter αN. It's convenient to not simply use α as the varying value since the most interesting part of the plot is close to $\alpha N = 1$. This is motivated by results of the Bogoliubov approximation and it breaking down at $\alpha N = 1$ [10]. Typically the energy spectrum narrows at this point before spreading out again. We can clearly see that the energy spectrum narrows when αN reaches a certain point close to one and that the energies tend to collapse on the ground state or at least get a lot more dense. Both are indicators for a quantum phase transition.

In figure (1), the number of particles is fixed, but we can see the exact behavior for a fixed α, as seen in figure (2).

In order to further investigate the properties of the system close to the critical αN, it is beneficial to keep αN constant while varying the number of particles N. In other words, we choose a value of αN in figure (1) and observe the energy differences while varying the number of particles of the system.

To better visualize what happens to the plot (3) when going through different values of αN, we choose a certain exited energy and display a contour plot as a function of αN and N in figure (4).

We can see in figure (4) that as the number of particles increases the minimum in the energy gap decreases and shifts closer to $\alpha N = 1$.

This means that as the system gets bigger, i.e., the number of particles of the system

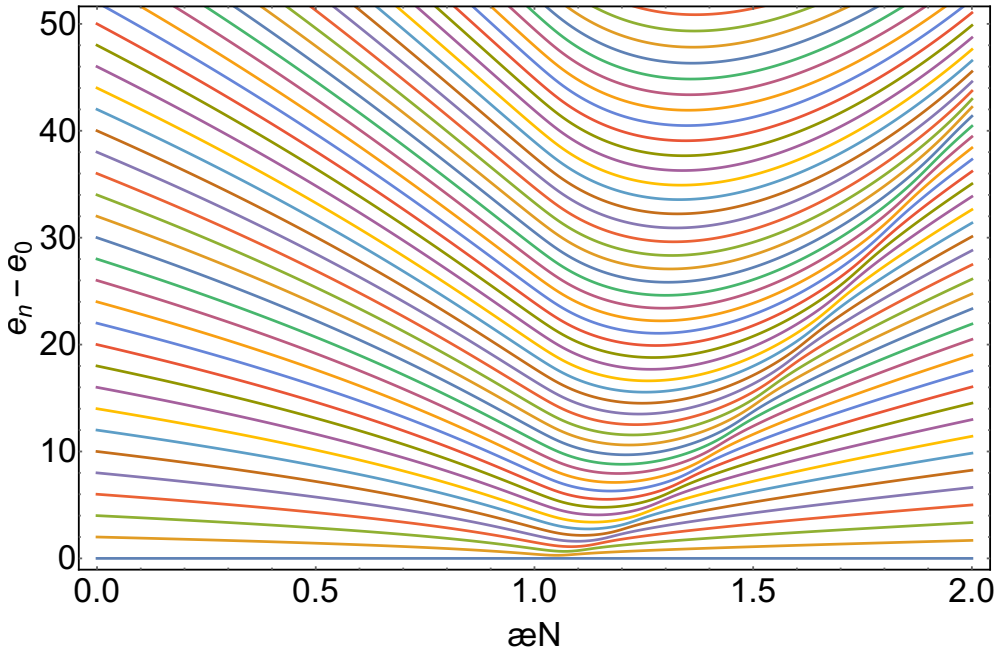

Figure 1: Energy difference narrows around the critical point and a strongly inhomogeneous density of states after the critical point $\alpha N = 1$.
$(N = 300, L = 0)$

increases, a lower coupling constant is sufficient to reach the critical point, but not only because N trivially increases in the coupling parameter αN.
It also implies that the system at the critical point is easier to excite since the excitation energy lowers.
We will look at this phenomena more quantitatively in chapter 4.1.

3.1. Five-site-case for arbitrary L and parabolic dispersion relation

The next natural step is to expand the truncation, so to go from three to five sites. We consider again the same Hamiltonian (7) as in the chapter before, but allow the values of the k-mode to range from -2 to 2 instead of -1 to 1.
The most obvious difference when comparing figure (5) with (1) is the possible occurrence of crossings in the excitation spectrum for fixed L and N.
Crossings are an indicator of a locally conserved quantity. In order to verify crossings and thus exclude avoided crossings, we have to look closely at the crossing point. The intersection one marked in figure (5) turns out to be an avoided crossing as we can see in figure (6).
The intersection two also seems to be an avoided crossing as seen in figure (7). Since we can not find any crossings, it is likely that this model doesn't have any more integrals of motion that we could exploit to reduce the systems phase space.

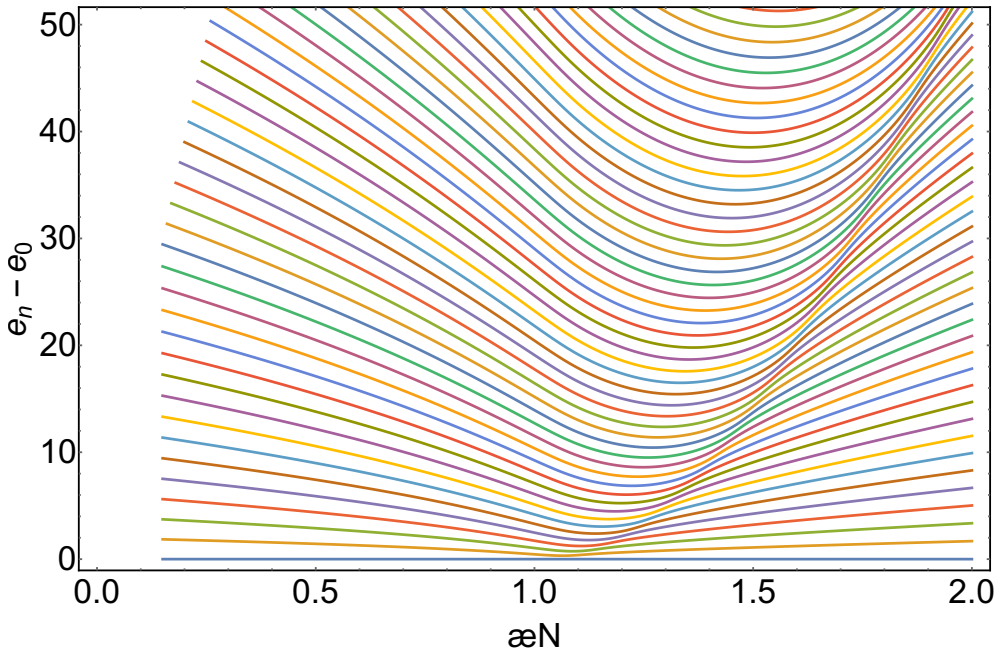

Figure 2: Same behavior as in figure (1) when varying N.
($\alpha = 0.005, L = 0, N = 30 - 400$)

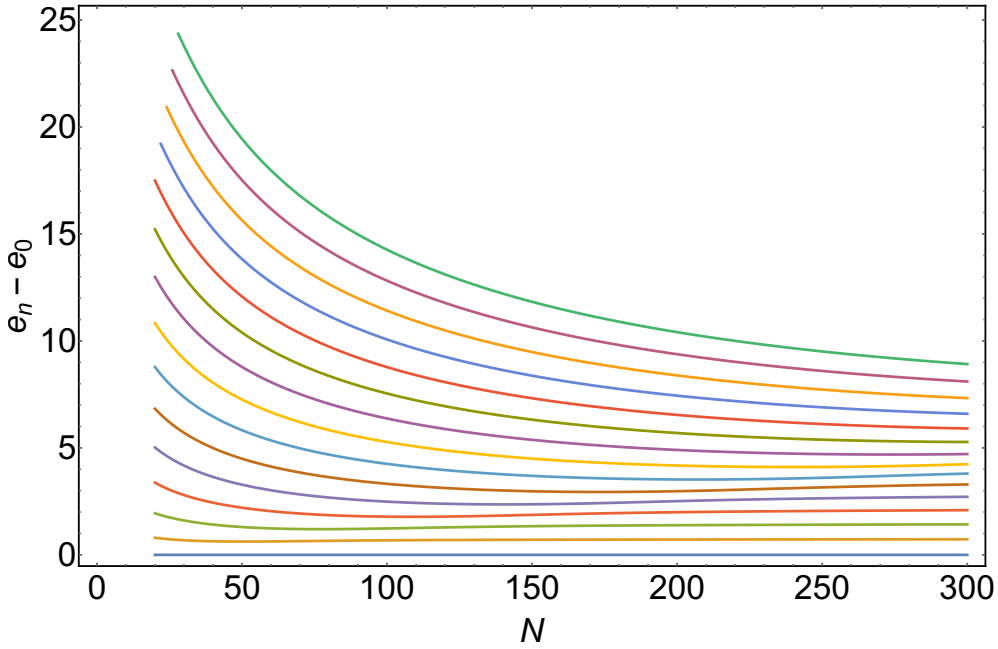

Figure 3: Energy difference while varying N and keeping αN fixed.
($N = 20 - 300, L = 0, \alpha N = 1.25$)

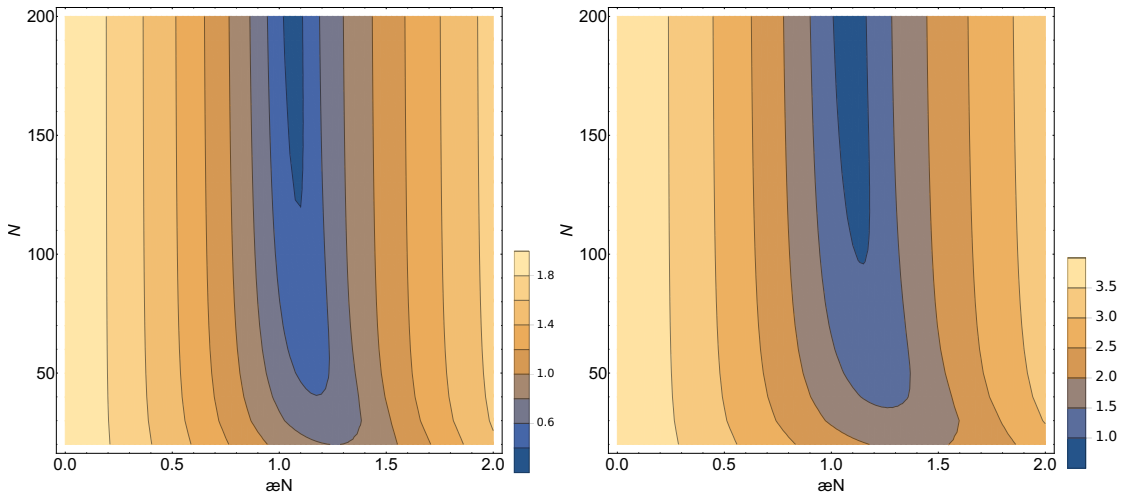

Figure 4: Energy difference between the first exited state and ground state (left) and second exited state and ground state (right). Energy minimum shifting closer to $\alpha N = 1$ and getting lower with an increasing amount of particles.

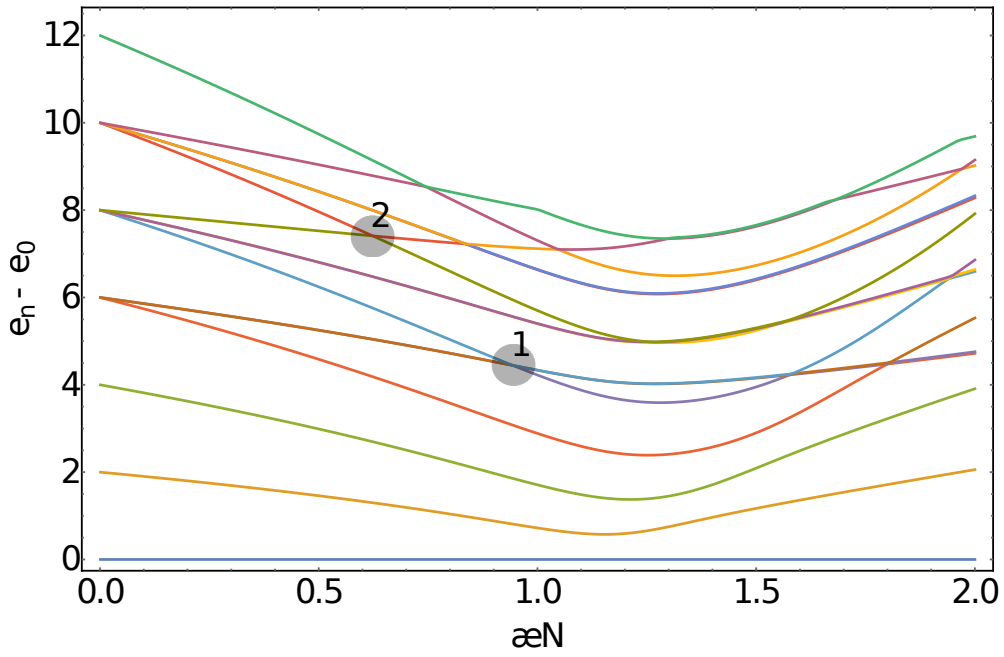

Figure 5: Plot of the energy difference for the 5-site-case with parabolic dispersion relation - two crossings are marked.
$(N = 30, L = 0, n_{max} = 15)$

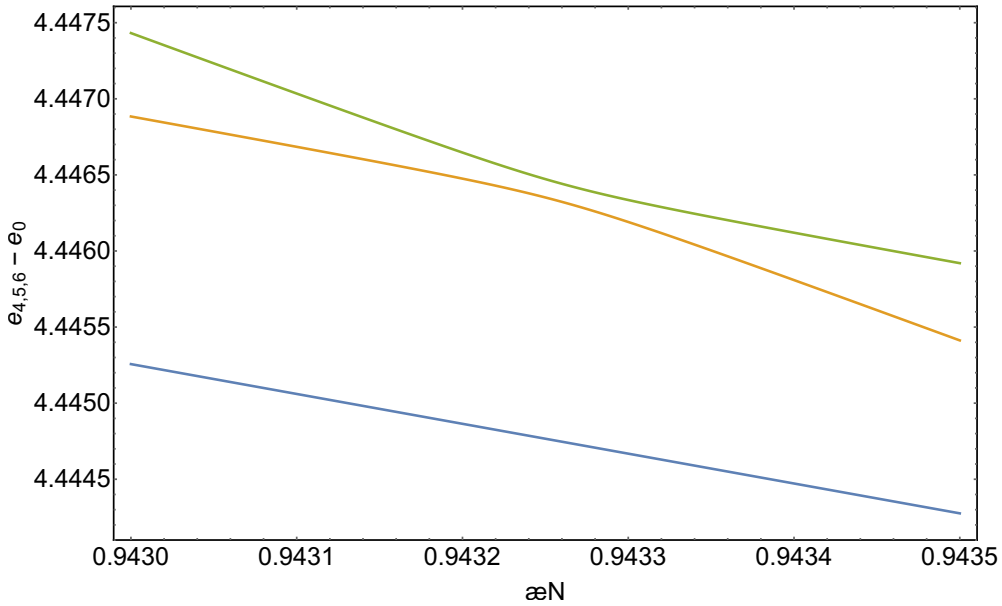

Figure 6: Zoom in near the crossing point one. No indication of unused integrals of motion through this crossing since it is an avoided crossing.

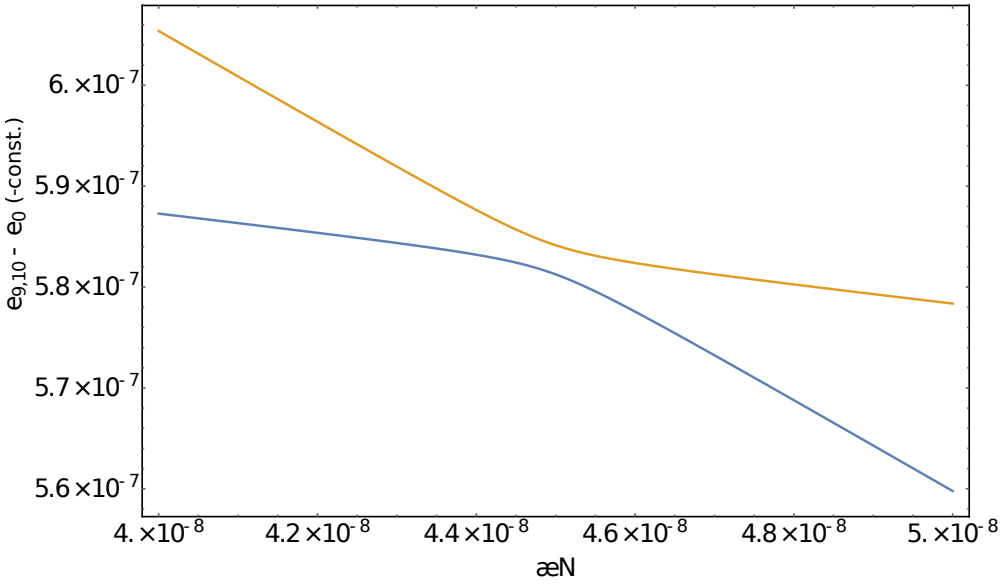

Figure 7: Zoom in near the crossing point two and the crossing turns out to be (again) an avoided crossing.

4. Five-site-case for arbitrary L and linear dispersion relation

We now only change the parabolic dispersion relation in the Hamiltonian from last chapter and replace it by a linear one, but leave everything else unchanged.
This has the advantage that we can compare the functional dependence on the number of particles of quantities like the gap-energy and -position to the functional dependences in the five-site-case with parabolic dispersion relation, because, in the parabolic case, they have already been approximated in the following PhD thesis [11].
These quantities are meaningful, since we are interested in finding quantum phase transitions - but quantum phase transitions occur in large systems, ideally $N \to \infty$. So, it's important to examine how the indicators of a quantum phase transitions change when going from small to large systems, e.g., if the (assumed) signs for a quantum phase transition disappear when increasing the system size, then there is no phase transition after all.
Thus, we review the model given by the Hamiltonian (with $\frac{\hbar}{2m} = 1$ and $R = 2\pi$)

$$H = \sum_{k=\pm 2,\pm 1,0} |k| a_k^\dagger a_k - \alpha \sum_{k,l,m,n=\pm 2,\pm 1,0} \delta_{k+l,m+n} a_k^\dagger a_l^\dagger a_m a_n. \tag{11}$$

Figure (8) is a plot of the n_{max} lowest energies of the system for different values of αN with N being the fixed number of particles. As mentioned earlier, it is convenient to not simply use α as the varying parameter since the most interesting part of the plot is close to $\alpha N = 1$ since if a quantum phase transition occurs, the energy spectrum narrows around this point.
This becomes even more visible when looking at the energy difference to the groundstate as seen in figure (9).

4.1. Gap-energy and -position of first and second exited energy

Comparing figure (9) and (10), we can see that with an increasing number of particles the extrema are getting lower and are shifting closer to one.
This is especially easy to see in figure (11) as only the first and second exited energies for different particle numbers are shown. In order to answer what the functional dependence on N of these behaviors is, we look at the first and second exited energy and plot the αN and $(e_{1/2} - e_0)$ values of the minimum against the number of particles N.
We define $\lambda_{1/2}$ and $u_{1/2}$ by

$$\begin{aligned} \frac{\partial (e_{1/2} - e_0)}{\partial \alpha N}\Big|_{\alpha N = \lambda_{1/2}} &= 0, \\ u_{1/2} = (e_{1/2} - e_0)\Big|_{\lambda_{1/2}} & \end{aligned} \tag{12}$$

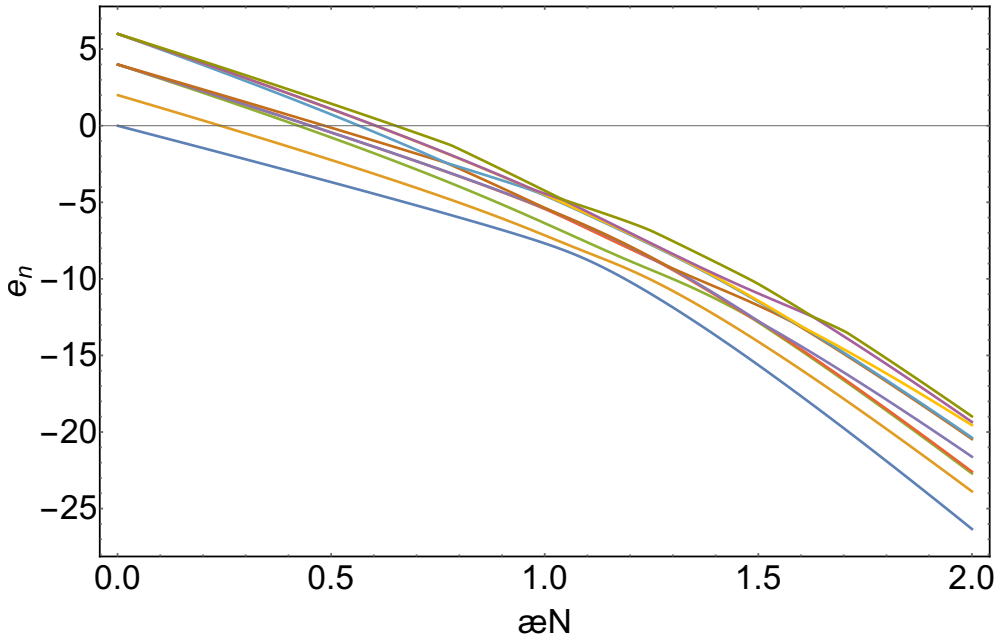

Figure 8: Ten lowest energies as a function of αN.
$(N = 30, L = 0, n_{max} = 10)$

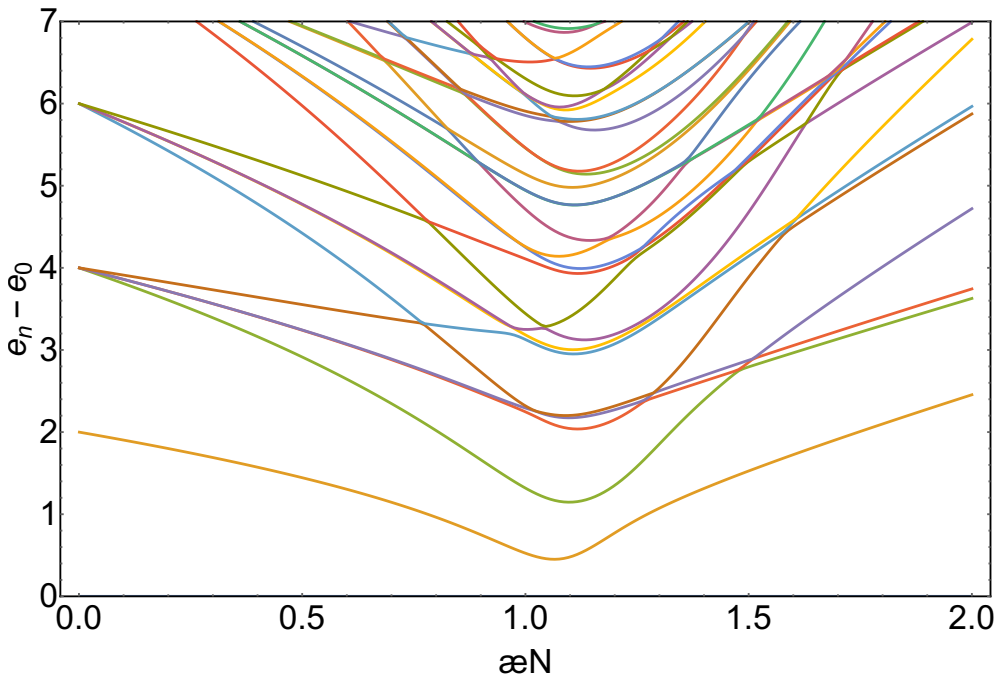

Figure 9: Ten lowest energy differences as a function of αN.
$(N = 30, L = 0)$

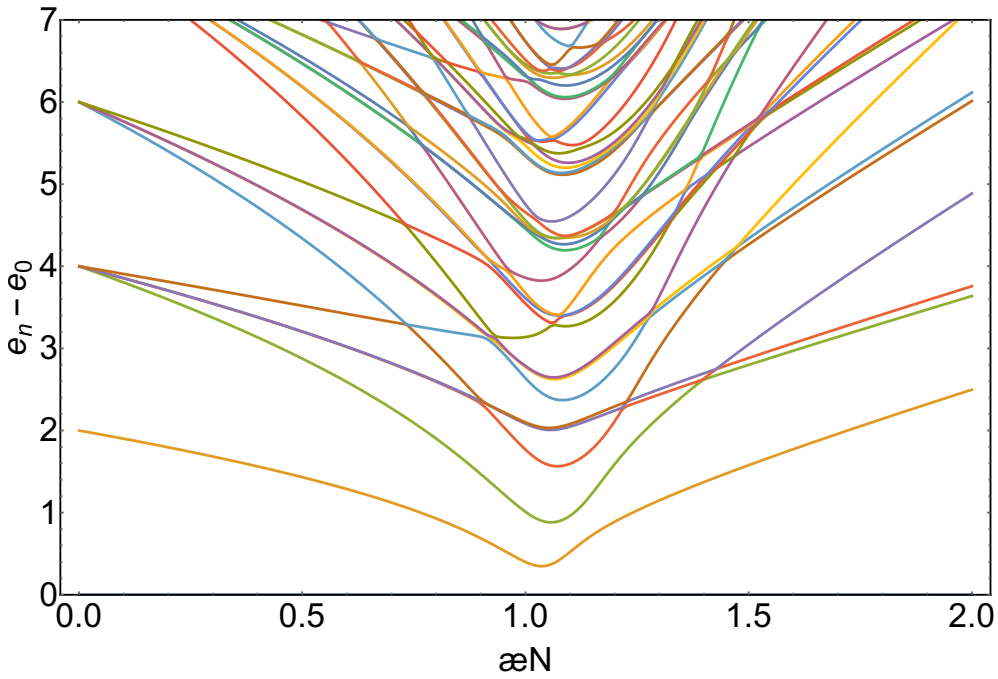

Figure 10: Ten lowest energy differences as a function of αN.
$(N = 50, L = 0)$

and assume a relation of the form

$$\lambda = N^m \qquad \Big| \log()$$
$$\log(\lambda) = \log(N^m) = m \log(N),$$

so the slope of the double logarithmic plot is our exponent m.
This results in the parameters and figures (12-15)

$$\lambda_1 \propto N^{-1.50841},$$

$$u_1 \propto N^{-0.524327},$$

$$\lambda_2 \propto N^{-1.47971},$$

$$u_2 \propto N^{-0.51829}.$$

In the five-site-case with parabolic dispersion relation these dependences are [11]

$$u_{\text{semiclassic}} \propto N^{-\frac{1}{3}},$$
$$\lambda_{\text{semiclassic}} \propto N^{-\frac{2}{3}}.$$

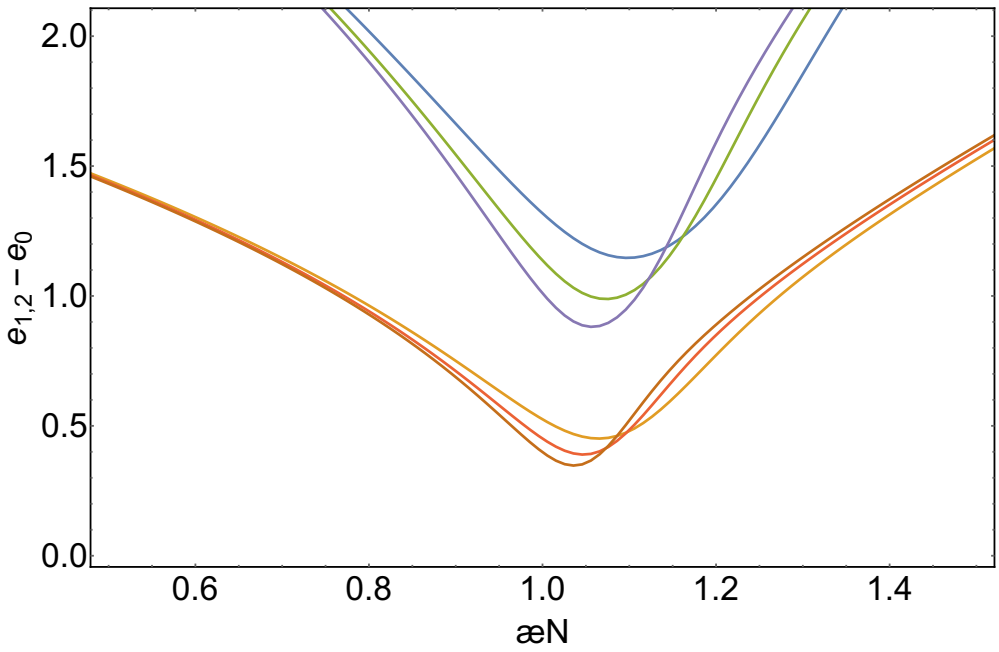

Figure 11: First and second exited energy for three different particle numbers. The minimum is getting lower and shifts towards the critical point for an increasing number of particles.
($N = 30, 40, 50; L = 0; n = 1, 2$)

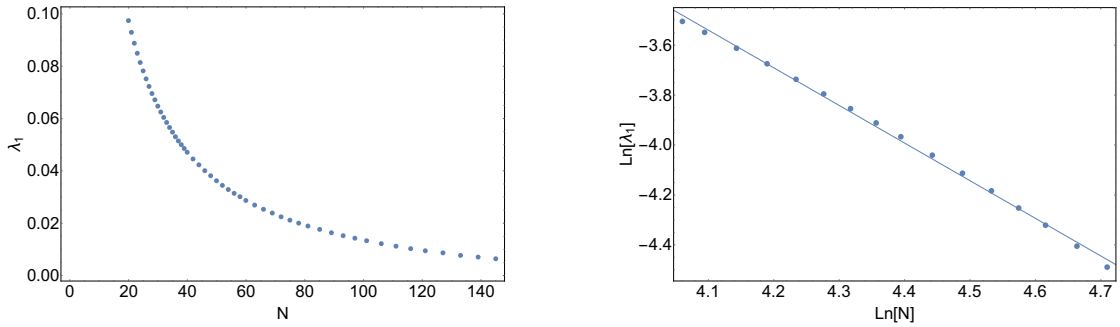

Figure 12: αN value of the first exited energy minimum as a function of the number of particles in order to determine the linear fit parameters:
$2.64476 - 1.50841x$

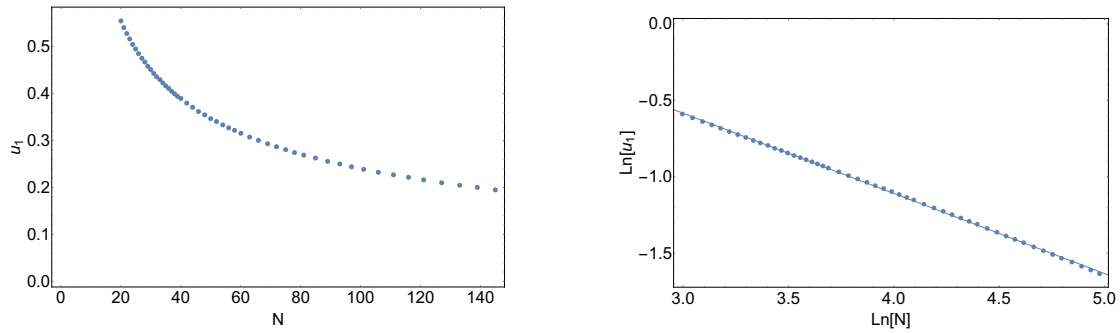

Figure 13: Energy value of the first exited energy minimum as a function of the number of particles in order to determine the linear fit parameters:
$0.988412 - 0.524327x$

Theses dependences differ from the five-site-case with linear dispersion relation. Therefore, replacing the parabolic- by a linear dispersion relation does make a difference in that regard.

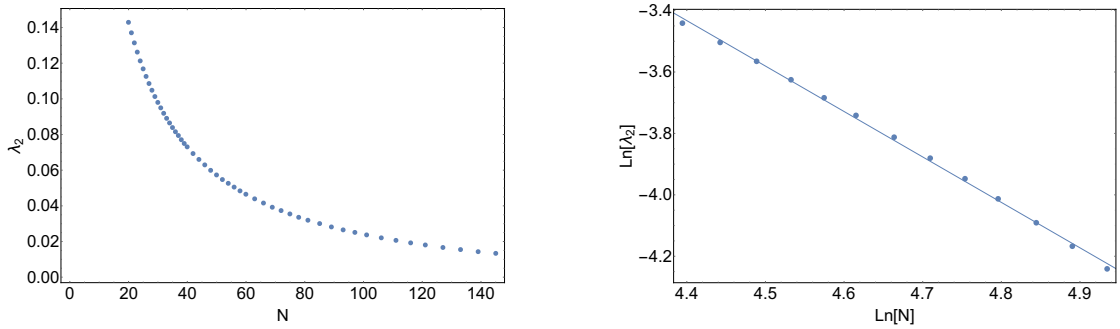

Figure 14: αN value of the second exited energy minimum as a function of the number of particles in order to determine the linear fit parameters:
$3.07803 - 1.47971x$

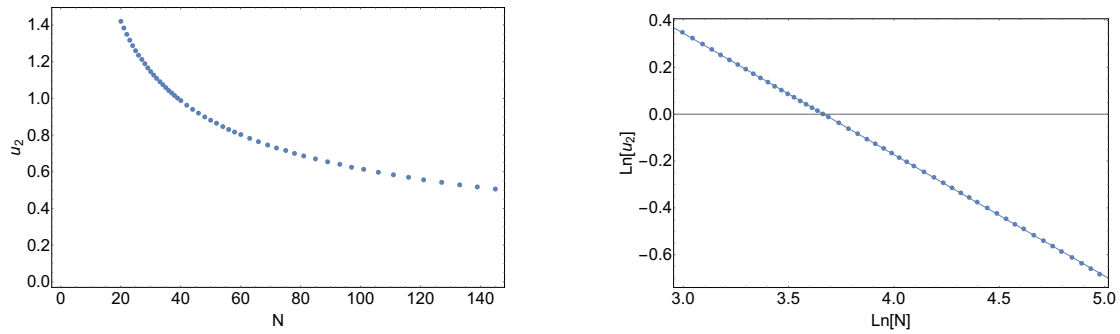

Figure 15: Energy value of the second exited energy minimum as a function of the number of particles in order to determine the linear fit parameters:
$1.90059 - 0.51829x$

5. Three-site-case for arbitrary L with spin 1/2 and linear dispersion relation

Now, we go one step further and also allow negative energies, and look at a model where we essentially assume our bosons to have some form of (quasi-)spin-$\frac{1}{2}$ - for example a bosonic system with two energy bands. In the environment of a crossing of the two dispersion relations it can be approximated as a linear relation.
This is an entirely new system and only shares similarities with the Lieb-Liniger model. Another possible interpretation of the subsequently defined Hamiltonian is that massless particles have, in the moment the interaction occurs, a mass, creating a gap between negative and positive energies.

$E(k,s) = sk$ with $s \in \{\pm 1\}$

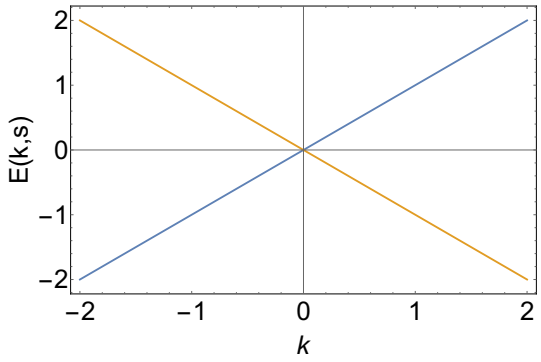

The Hamiltonian in first quantization is defined as

$$H = \frac{-i\hbar}{2m}\sum_{\alpha=1}^{N}\frac{\partial}{\partial x_\alpha}\sigma_x^{(\alpha)} - 2R\alpha\sum_{\alpha\neq\beta,\alpha<\beta}\delta(x_\alpha - x_\beta)(\sigma_z^{(\alpha)}\otimes\sigma_z^{(\beta)}) \tag{13}$$

and in second quantization

$$\begin{aligned} H = &\frac{-i\hbar}{2m}\sum_{\substack{k,k'=\pm1,0\\ \sigma,\sigma'=\pm}}\langle k|\frac{\partial}{\partial x}|k'\rangle\,\langle\sigma|\sigma_x|\sigma'\rangle\,a_{k\sigma}^\dagger a_{k'\sigma'} \\ &- R\alpha\sum_{\substack{k,l,m,n=\pm1,0\\ \sigma,\sigma',\gamma,\gamma'=\pm}}\langle k,l|\delta(x-x')|n,m\rangle\,\langle\sigma,\sigma'|\sigma_z^{(1)}\otimes\sigma_z^{(2)}|\gamma',\gamma\rangle\,a_{k\sigma}^\dagger a_{l\sigma'}^\dagger a_{m\gamma}a_{n\gamma'} \end{aligned}$$

where $a_{k,\sigma}^\dagger$ and $a_{k,\sigma}$ are the annihilation- and creation-operator

$$a_{k,\sigma}^\dagger|\Omega\rangle = |k,\sigma\rangle_\alpha\,,\; a_{k,\sigma}|k,\sigma\rangle_\alpha = |\Omega\rangle\,,\; a_{k,\sigma}|\Omega\rangle = 0. \tag{14}$$

$|\Omega\rangle$ is the vacuum state. They also satisfy the commutator relations

$$\begin{aligned} [a_{k\sigma}, a_{k'\sigma'}^\dagger] &= \delta_{k,k'}\delta_{\sigma,\sigma'}, \\ [a_{k\sigma}, a_{k'\sigma'}] &= [a_{k\sigma}^\dagger, a_{k'\sigma'}^\dagger] = 0. \end{aligned}$$

Since we chose the kinetic term of the Hamiltonian to be proportional to σ_x, the two spin states are

$$|\pm\rangle = \frac{1}{\sqrt{2}} \begin{pmatrix} 1 \\ \pm 1 \end{pmatrix}. \tag{15}$$

This allows us to calculate the following matrix elements

$$\langle \sigma, \sigma' | \sigma_z^{(1)} \otimes \sigma_z^{(2)} | \gamma', \gamma \rangle = \langle \sigma | \sigma_z | \gamma' \rangle \langle \sigma' | \sigma_z | \gamma \rangle = \begin{cases} 1 & \sigma\sigma'\gamma'\gamma \in M \\ 0 & \text{else} \end{cases},$$
$$\text{where } M = \{++--, --++, +--+, -++-\}$$

$$\langle \sigma | \sigma_x | \sigma' \rangle = \begin{cases} 1 & \sigma\sigma' \in \{++, --\} \\ 0 & \text{else} \end{cases}, \qquad \langle k | \frac{\partial}{\partial x} | k' \rangle = i \frac{2\pi}{R} k' \delta_{k,k'}.$$

So the Hamiltonian of the system becomes (with $\frac{\hbar}{2m} = 1$ and $R = 2\pi$)

$$H = a_{1+}^\dagger a_{1+} - a_{1-}^\dagger a_{1-} - a_{-1+}^\dagger a_{-1+} + a_{-1-}^\dagger a_{-1-} - \alpha \Big[\sum_{\substack{k,l,m,n=\pm 1,0 \\ \sigma \neq \gamma}} \delta_{k+l,m+n} \left(a_{k\sigma}^\dagger a_{l\sigma}^\dagger a_{m\gamma} a_{n\gamma} + a_{k\sigma}^\dagger a_{l\gamma}^\dagger a_{m\sigma} a_{n\gamma} \right) \Big] \tag{16}$$

$$\underset{\substack{\uparrow \\ \text{Appendix A}}}{=} H_0 - \alpha \left(H_{diag} + H_{offdiag} + H_{offdiag}^\dagger \right) \tag{17}$$

with

$$H_0 = n_{1+} - n_{1-} - n_{-1+} + n_{-1-}, \tag{18}$$

$$H_{diag} = 2 \sum_{k=\pm 1,0} \Big[n_{k+} n_{k-} + \sum_{\substack{l=\pm 1,0 \\ l>k}} (n_{k+} n_{l-} + n_{k-} n_{l+}) \Big], \tag{19}$$

$$H_{offdiag} = \sum_{\substack{k,l=\pm 1,0 \\ k<l}} \left(4 a_{k+}^\dagger a_{l+}^\dagger a_{k-} a_{l-} + 2 a_{k+}^\dagger a_{l-}^\dagger a_{l+} a_{k-} \right) + \sum_{k=\pm 1,0} a_{k+}^\dagger a_{k+}^\dagger a_{k-} a_{k-} + \sum_{\sigma \neq \gamma} 2 \left(a_{1\sigma}^\dagger a_{-1\sigma}^\dagger a_{0\gamma} a_{0\gamma} + a_{1\sigma}^\dagger a_{-1\gamma}^\dagger a_{0\sigma} a_{0\gamma} \right). \tag{20}$$

The strategy is now again to write this Hamiltonian in some basis, diagonalize it and plot its lowest energies as functions of the coupling constant α. As a basis we may choose

$$|n_{1+}, n_{0+}, n_{-1+}, n_{1-}, n_{0-}, n_{-1-}\rangle = |n_1, n_2, n_3, n_4, n_5, n_6\rangle. \tag{21}$$

To evaluate the Hamiltonian, we need to make an enumerated list of all allowed states for a given N and L. This is simply a generalization of the three-site-case. As an example equation (8) and (10) gives us, for $N = 2$ and $L = 1$, only one allowed state being

$$|n_1 = 1, n_0 = 1, n_{-1} = 0\rangle = |1, 1, 0\rangle.$$

In the case here this would relate to four allowed states:

$$|0,0,0,1,1,0\rangle\,, |0,1,0,1,0,0\rangle\,, |1,0,0,0,1,0\rangle\,, |1,1,0,0,0,0\rangle$$

We rearrange this in our state list in the form

$$stateList_{ij} = n_{ij} \text{ with } \tfrac{i=1..d}{j=1..6}.$$

Thus, the dimension of the Hamiltonian matrix and length of the state list d is given by

$$\begin{aligned} d &= \sum_{n=0}^{\lfloor\frac{N-L}{2}\rfloor} (n+1)(N-L-2n+1)(L+n+1) \qquad (22)\\ &= -\frac{1}{6}\Big((1+f)(2+f)(-3+3f+3f^2+6fL+3L^2-3N-2fN-3LN)\Big) \propto N^4 \\ &\qquad\qquad \text{with } f = \lfloor\frac{N-L}{2}\rfloor. \end{aligned}$$

Now, we can start to calculate the Hamiltonian matrix

$$H_{kj} = \langle k|H|j\rangle = \langle k|H_0|j\rangle - \alpha\left(\langle k|H_{diag}|j\rangle + \langle k|H_{offdiag}|j\rangle + \langle k|H^\dagger_{offdiag}|j\rangle\right)$$

with

$$|j\rangle = |n_{j1}, n_{j2}, n_{j3}, n_{j4}, n_{j5}, n_{j6}\rangle\,. \qquad (23)$$

We examine the off-diagonal matrix first

$$\langle k|H_{offdiag}|j\rangle = \langle k|\sum_{i=1}^{13} c_i f_i n_i|j\rangle = \sum_{i=1}^{13} c_i n_i(j)\,\langle k|f_i|j\rangle \qquad (24)$$

where i is an arbitrary numbering of the thirteen terms of $H_{offdiag}$. For instance, one of the terms is $4a_1^\dagger a_2^\dagger a_4 a_5$ and, as an example, would relate to

$$\begin{aligned} c &= 4,\\ n(j) &= \sqrt{(n_{j1}+1)(n_{j2}+1)n_{j4}n_{j5}},\\ f\,|j\rangle &= |n_{j1}+1, n_{j2}+1, n_{j3}, n_{j4}-1, n_{j5}-1, n_{j6}\rangle \end{aligned}$$

and analog for the rest.
In the sum of equation (24), only one of the thirteen terms of $H_{offdiag}$ will deliver a contribution unequal to zero. For practical purposes it is more efficient to define and use a tensor of rank six given by

$$G_{n_{i1},n_{i2},n_{i3},n_{i4},n_{i5},n_{i6}} = i \text{ and } = 0 \text{ when not specified.} \qquad (25)$$

This enables to quickly check if any given set of occupation numbers

$$|k'\rangle = |n_1^{k'}, n_2^{k'}, n_3^{k'}, n_4^{k'}, n_5^{k'}, n_6^{k'}\rangle$$

is part of the state list, i.e., is an allowed state of the system and, if so, at which position it is in the state list.
For example, if we look at a particular term of the the off-diagonal Hamiltonian acting on $|j\rangle$

$$c_1 n_1 f_1 |j\rangle = c_1 n_1(j) |k'\rangle ,$$

it will deliver us a matrix element at position

$$H_{G_{n_1^{k'},n_2^{k'},n_3^{k'},n_4^{k'},n_5^{k'},n_6^{k'},j}} = c_1 n_1(j) \text{ if } G_{n_1^{k'},n_2^{k'},n_3^{k'},n_4^{k'},n_5^{k'},n_6^{k'}} \neq 0.$$

This approach reduces the amount of calculation needed for the off-diagonal part from $13d^2$ to $13d$.
The diagonal part of the Hamiltonian is trivial and given by

$$H_{0_{kk}} = n_{k1} - n_{k3} - n_{k4} + n_{k6},$$

$$H_{diag_{kk}} = 2\Big(n_{k1}n_{k4} + n_{k2}n_{k5} + n_{k3}n_{k6} + n_{k2}n_{k4} + n_{k5}n_{k1} + n_{k3}n_{k5} + n_{k6}n_{k2} + n_{k3}n_{k4} + n_{k6}n_{k1}\Big). \quad \text{for } k = 1..d \quad (26)$$

5.1. Example: Hamiltonian matrix for (N, L) = (2,1) and (3,2)

To get a feeling for the structure of the matrix, they are written here in full form for two examples with a low-dimensional state space.

$$H[2,1] = \underbrace{\begin{pmatrix} -1 & 0 & 0 & 0 \\ 0 & -1 & 0 & 0 \\ 0 & 0 & 1 & 0 \\ 0 & 0 & 0 & 1 \end{pmatrix}}_{H_0} - \alpha \left[\underbrace{\begin{pmatrix} 0 & 0 & 0 & 0 \\ 0 & 2 & 0 & 0 \\ 0 & 0 & 2 & 0 \\ 0 & 0 & 0 & 0 \end{pmatrix}}_{H_{diag}} + \underbrace{\begin{pmatrix} 0 & 0 & 0 & 4 \\ 0 & 0 & 2 & 0 \\ 0 & 2 & 0 & 0 \\ 4 & 0 & 0 & 0 \end{pmatrix}}_{H_{offdiag}+H_{offdiag}^{\dagger}} \right]$$

$$H[3,2] = \begin{pmatrix} -2 & 0 & 0 & 0 & 0 & 0 \\ 0 & -2 & 0 & 0 & 0 & 0 \\ 0 & 0 & 0 & 0 & 0 & 0 \\ 0 & 0 & 0 & 0 & 0 & 0 \\ 0 & 0 & 0 & 0 & 2 & 0 \\ 0 & 0 & 0 & 0 & 0 & 2 \end{pmatrix} - \alpha \begin{pmatrix} 0 & 0 & 0 & 0 & 0 & 0 \\ 0 & 4 & 0 & 0 & 0 & 0 \\ 0 & 0 & 4 & 0 & 0 & 0 \\ 0 & 0 & 0 & 4 & 0 & 0 \\ 0 & 0 & 0 & 0 & 4 & 0 \\ 0 & 0 & 0 & 0 & 0 & 0 \end{pmatrix}$$

$$- \alpha \begin{pmatrix} 0 & 0 & 0 & 5.65685 & 2 & 0 \\ 0 & 0 & 2.82843 & 0 & 0 & 2 \\ 0 & 2.82843 & 0 & 0 & 0 & 5.65685 \\ 5.65685 & 0 & 0 & 0 & 2.82843 & 0 \\ 2 & 0 & 0 & 2.82843 & 0 & 0 \\ 0 & 2 & 5.65685 & 0 & 0 & 0 \end{pmatrix}$$

5.2. Critical point

In the previous chapters we observed the critical point for the combined parameter αN to be typically close to one. As we can see in figure (16) this point has now been shifted close to one half. Although it's questionable if the definition of a critical point really makes sense here, since when comparing the latter figure to, e.g., figure (1), the indicators for a quantum phase transitions are far less visible, i.e., if there is a quantum phase transition, then one can only suspect it.
The key problem is that, as mentioned earlier, phase transitions occur in large systems but while the dimension of the Hamiltonian matrix in the three-site-case with no spin degree of freedom grows $\propto N$, in our three-site-case with a spin degree of freedom it grows $\propto N^4$.
So, while in the system, whose energies are displayed in figure (1), 300 particles are manageable, in the system discussed in this chapter they aren't and consequently a quantum phase transition is a lot harder to find.

5.3. Symmetries/constants of motion

In, for example, figure (16) we can see several crossing and can, numerically, exclude avoided crossings with a precision of 10^{-16}.
Therefore, there are most likely still integrals of motions we should use to reduce the system's phase space. This makes sense because a constant of motion doesn't change per definition as the system defined by a certain Hamiltonian progresses. According to that the state of the system with a certain value of the constant of motion will never progress into a state with a different value of the same constant of motion. So, any state space with a certain value of a constant of motion is independent of the state space with any different value of this constant of motion. This guarantees us that, by fixing constants of motion, we only cut off states the system could never progress into in the first place.
For the system discussed in this chapter such an integral of motion is the operator $\hat{P}$.
The Hamiltonian given in (16) is invariant under the simultaneous swap of all spin- and

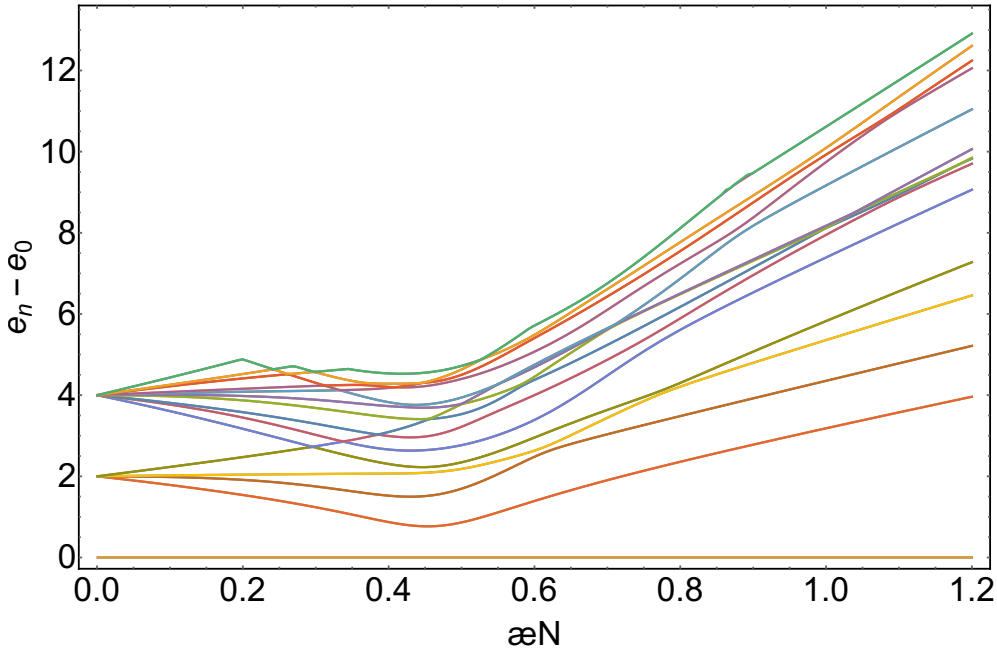

Figure 16: Energy difference to the groundstate as a function of αN. The critical point occurs at around $\alpha N = 0.5$.
$(N = 15, L = 0, n_{max} = 30)$

k-values. So, it is invariant under the operator:

$$\hat{P}\{k, \sigma\} \equiv \{-k, -\sigma\} \tag{27}$$

Using (21) and (23), it follows that

$$\hat{P}|i\rangle = \hat{P}|n_{i1}, n_{i2}, n_{i3}, n_{i4}, n_{i5}, n_{i6}\rangle = |n_{i6}, n_{i5}, n_{i4}, n_{i3}, n_{i2}, n_{i1}\rangle\,. \tag{28}$$

However, the resulting state in latter equation only has the same momentum for $L = 0$, since $L = -L \Leftrightarrow L = 0$.
It holds true that

$$\hat{P}\hat{P}|i\rangle = |i\rangle \Leftrightarrow \hat{P}|i\rangle = \pm|i\rangle\,,$$

$$H\hat{P}|i\rangle = \hat{P}H|i\rangle = \hat{P}E_i|i\rangle = E_i\hat{P}|i\rangle \Rightarrow H\left(|i\rangle \pm \hat{P}|i\rangle\right) = E_i\left(|i\rangle \pm \hat{P}|i\rangle\right).$$

So, we can transform into a new basis which is an eigenbasis of the operator $\hat{P}$ given by

$$|j\rangle_\pm \equiv \frac{1}{\sqrt{2}}\left(|i\rangle \pm \hat{P}|i\rangle\right) \text{ and } \hat{P}|j\rangle_\pm = \pm|j\rangle_\pm\,.$$

The transformation matrix for the basis change becomes

$$T_{ij} = \langle n_i | m_j\rangle \quad \forall i, j = 1...d \tag{29}$$

where $\{|m_i\rangle\}$ is the new basis and is arranged in a certain ordering

$$\left\{ |m_i\rangle \right\} = \left\{ |1\rangle_+ , .., |(d+W)/2\rangle_+ , |1\rangle_- , .., |(d-W)/2\rangle_- \right\} \tag{30}$$

with d given by (22) and W being the amount of state kets in the initial basis that are already eigenvectors of the operator $\hat{P}$.
W is, for $L = 0$,

$$W_N = \begin{cases} 0 & N \in 2\mathbb{N}+1 \\ W_{N-2} + \frac{N}{2} + 1 \text{ with } W_2 = 3 & N \in 2\mathbb{N} \end{cases} . \tag{31}$$

For Example for $N = 2$ and $L = 0$, there are seven allowed states (ket definition in (21)):

$$\Big\{ |0,0,0,0,2,0\rangle , |0,1,0,0,1,0\rangle , |0,2,0,0,0,0\rangle , \\ |0,0,0,1,0,1\rangle , |0,0,1,1,0,0\rangle , |1,0,0,0,0,1\rangle , |1,0,1,0,0,0\rangle \Big\}$$

The transformation matrix in this case then is

$$T = \frac{1}{\sqrt{2}} \begin{pmatrix} 0 & 0 & 0 & 1 & 0 & 1 & 0 \\ \sqrt{2} & 0 & 0 & 0 & 0 & 0 & 0 \\ 0 & 0 & 0 & 1 & 0 & -1 & 0 \\ 0 & 0 & 0 & 0 & 1 & 0 & 1 \\ 0 & \sqrt{2} & 0 & 0 & 0 & 0 & 0 \\ 0 & 0 & \sqrt{2} & 0 & 0 & 0 & 0 \\ 0 & 0 & 0 & 0 & 1 & 0 & -1 \end{pmatrix} . \tag{32}$$

The Hamiltonian matrix in the new basis has a two block structure

$$H[L=0] = \begin{pmatrix} H_+ & 0 \\ 0 & H_- \end{pmatrix} \tag{33}$$

with H_+ being of the dimension $\frac{d+W}{2} \times \frac{d+W}{2}$ and H_- being a $\frac{d-W}{2} \times \frac{d-W}{2}$ matrix. For an odd number of particles W is always zero.
In the structure of the Hamiltonian matrix in the new basis we can see what was mentioned earlier. The operator $\hat{P}$ has two eigenvalues ± 1, hence, the matrix in the new basis has two independent blocks, one for each eigenvalue.

5.4. Degeneracy for L=0 and odd number of particles

We can use this newly found constant of motion to try to understand the following phenomena.
For a small number of particles the dimension of the Hamiltonian matrix is reasonably low as well and thus enabling us to plot all eigenvalues. Figure (17) is such a plot of the full spectrum for $N = 3$ and $L = 0$.
From formula (22) we expect twelve eigenvalues, but can clearly only see six different

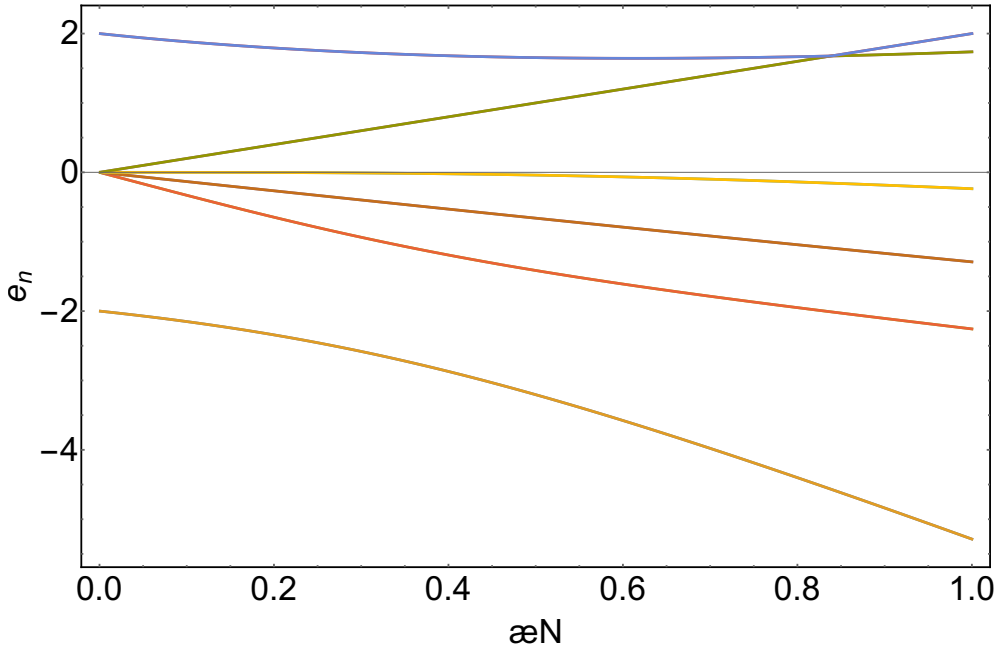

Figure 17: Full spectrum plot, i.e., plot of all eigenenergies for a given N, L. $(N = 3, L = 0, n_{max} = 12)$

curves in latter figure. After examining the data points themselves we find that every energy occurs with degeneracy two.
This degeneracy disappears when looking at a system with an even number of particles or if $L \neq 0$.
Taking a closer look at the Hamiltonian matrix given in (33), we find that the matrix H_+ has the same eigenvalues as H_- for an odd number of particles. Therefore H_- does not add any additional information of the system and initially choosing this basis and only calculating/diagonalizing H_+ greatly improves performance.

5.4.1. Kramers theorem

The above degeneracy for an odd number of particles can be explained by Kramers theorem.
Let θ be the time-reversal operator, so that $\theta |\alpha\rangle$ is the time-reversed state of $|\alpha\rangle$

$$\theta = K\hat{P} \tag{34}$$

with $\hat{P}$ defined in (27) and K being the complex conjugation.
One can show that

$$\theta^2(c_+ |+\rangle + c_- |-\rangle) = -(c_+ |+\rangle + c_- |-\rangle) \Leftrightarrow \theta^2 = -1 \tag{35}$$

holds true for a general spin $\frac{1}{2}$-ket (for a proof you may look in chapter 4.4 of [5]). This statement can be generalized to:

$$\theta^2 \left|j \text{ half-integer}\right\rangle = - \left|j \text{ half-integer}\right\rangle \tag{36}$$

If the commutator of H and θ vanishes, both energy eigenkets $|n\rangle$ and $\theta |n\rangle$ belong to the same energy eigenvalue. Assume $|n\rangle$ and $\theta |n\rangle$ represent the same state, thus they only differ by a phase factor

$$\theta |n\rangle = e^{i\delta} |n\rangle . \tag{37}$$

Applying θ from the left to latter equation results in

$$\theta^2 |n\rangle = \theta e^{i\delta} |n\rangle = e^{-i\delta}\theta |n\rangle = e^{-i\delta}e^{i\delta} |n\rangle = |n\rangle . \tag{38}$$

Which is a contradiction to equation (36) for half-integer j systems. Hence, the assumption was wrong and the two kets do not represent the same state - there must be a degeneracy. Furthermore, the degree of degeneracy is an even number[5].
This degeneracy is broken if we add a magnetic field, i.e., add

$$\sum_{\alpha=1}^{N} \beta \sigma_x^{(\alpha)} \tag{39}$$

to the Hamiltonian in (13) which simply favors configurations with an overall spin down[3].
Comparing figure (17) and (18) we can clearly see the degeneracy being broken by Zeeman splitting.

5.5. Full spectrum for $N = 2, 3, 4, 5$

Now, we can exploit the conservation of the time-reversal operator to reduce the system's phase space. We split the entire spectrum now in the two individual spectra defined by (33) and plot the eigenvalues for each matrix H_+, H_- in figures (19) to (22). We can again confirm the degeneracy for an odd number of particles as already discussed in the previous chapter in figure (20) and (22).
For $N = 2$ the Hamiltonian matrix suffices a more special form, and one can look at three independent blocks H', H_+, H_-:

$$H[L = 0, N = 2] = \begin{pmatrix} H' & 0 & 0 \\ 0 & H_+ & 0 \\ 0 & 0 & H_- \end{pmatrix} \tag{40}$$

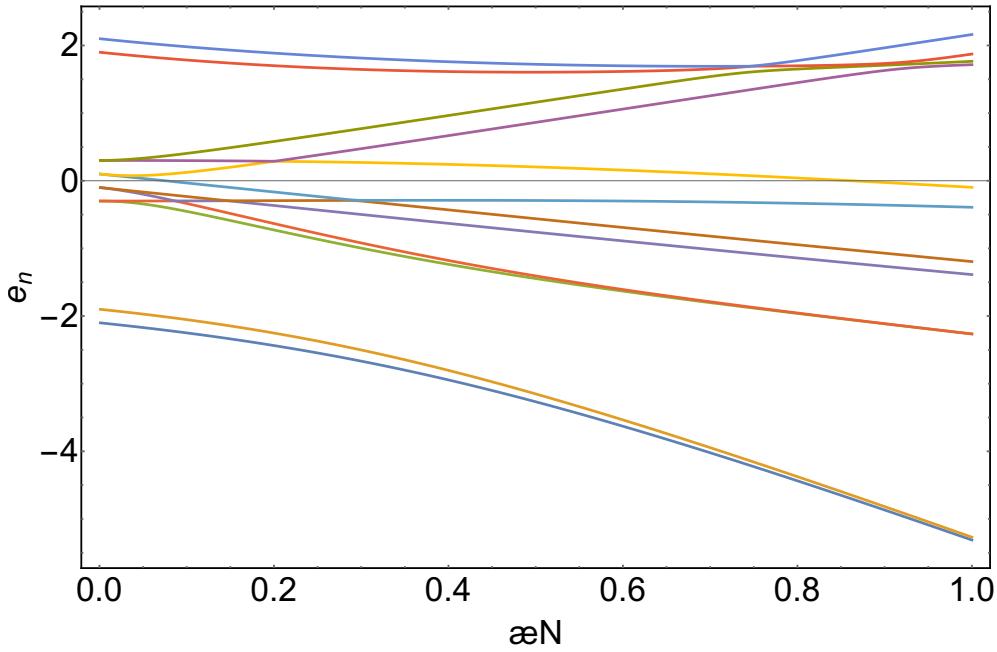

Figure 18: Full spectrum plot - the degeneracy is broken by the presence of a magnetic field.
($N = 3, L = 0, \beta = 0.1, n_{max} = 12$)

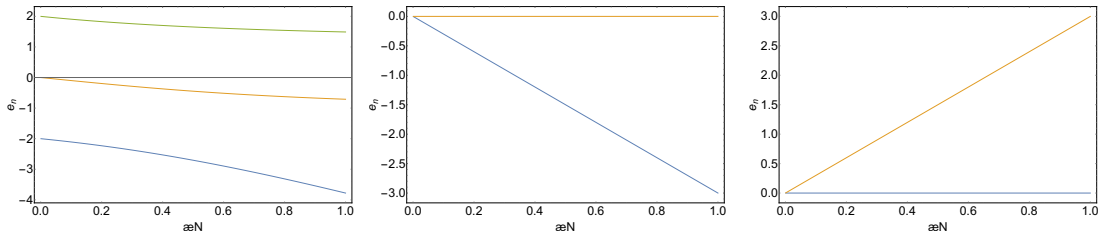

Figure 19: Plot of all eigenvalues of H', H_+, H_- for $N = 2$ particles - from left to right.

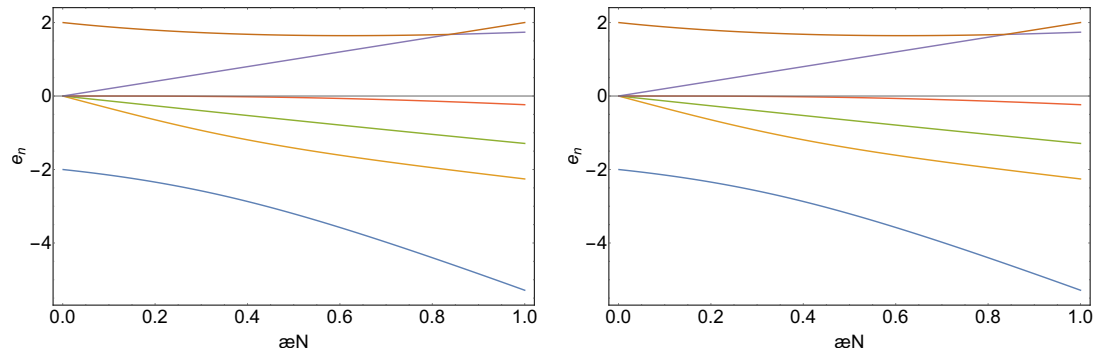

Figure 20: Plot of all eigenvalues of H_+, H_- for $N = 3$ particles - from left to right. Both plots are, due to the energy degeneracy for a system with an odd number of particles, identical.

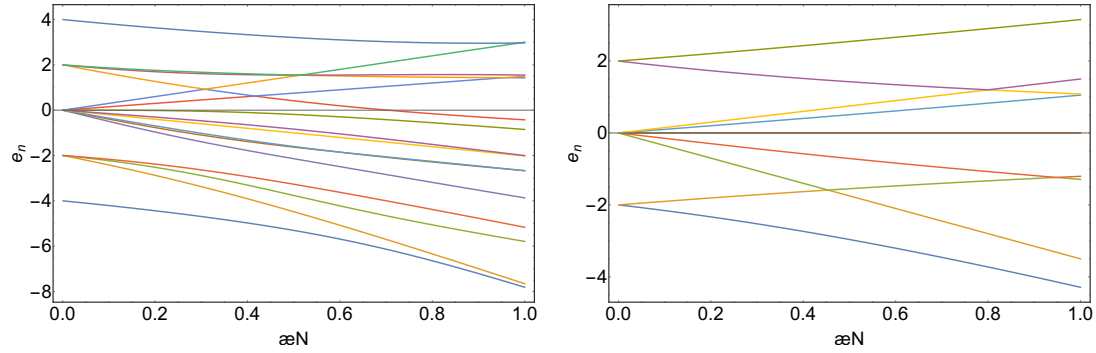

Figure 21: Plot of all eigenvalues of H_+, H_- for $N = 4$ particles - from left to right.

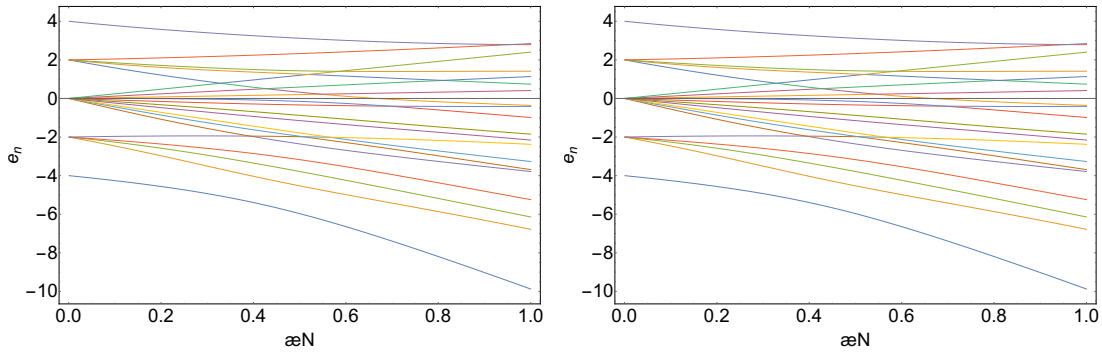

Figure 22: Plot of all eigenvalues of H_+, H_- for $N = 5$ particles - from left to right. Both plots are, due to the energy degeneracy for a system with an odd number of particles, identical.

5.6. Occurrence of energy crossings with fixed N, L, P

Taking a closer look at the right plot in figure (21) reveals an interesting crossing which is marked in figure (23). Since we are dealing with a system with a fixed number of particles, constant total momentum L and a fixed eigenvalue of the operator $\hat{P}$ given in expression (27), the occurence of a crossing is an indicator for another yet unused integral of motion.
As the energy gap between the two energies becomes smaller than 10^{-16}, which is machine-precision, it is relatively safe to exclude an avoided crossing. So, we conclude that there still might be some unused symmetry of the Hamiltonian.

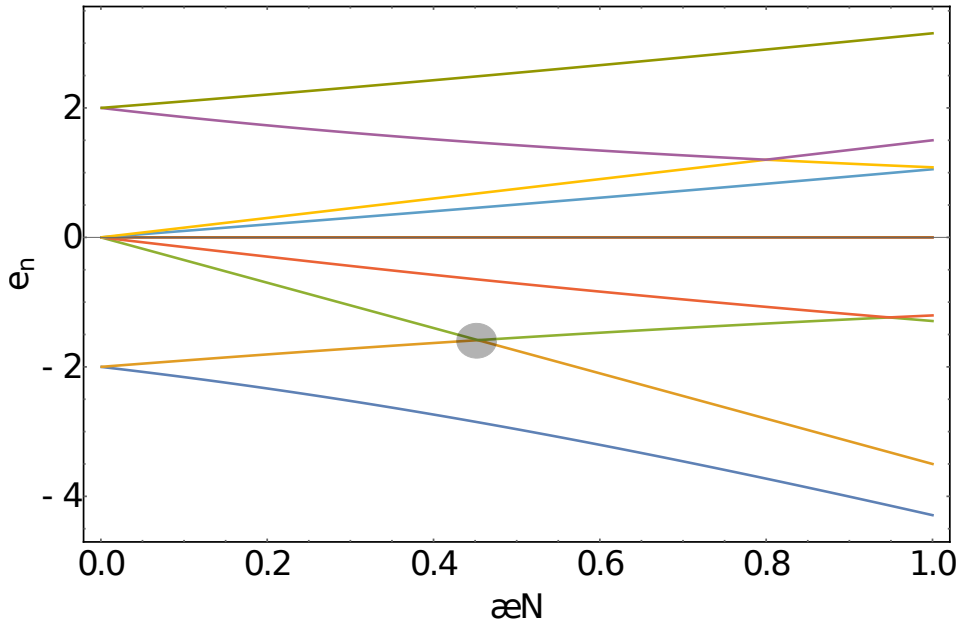

Figure 23: Plot of all eigenvalues of H_- for $N = 4$ and $L = 0$.

5.6.1. Product of spin operators as an integral of motion

The Hamiltonian in equation (13) is invariant under the operator $\hat{S}$ defined as

$$\hat{S} = \bigotimes_{\alpha=1}^{N} \sigma_x^{(\alpha)}. \tag{41}$$

The action of $\hat{S}$ on any ket defined by equation (21) is

$$\hat{S}\,|n_1, n_2, n_3, n_4, n_5, n_6\rangle = (-1)^{(n_4+n_5+n_6)}\,|n_1, n_2, n_3, n_4, n_5, n_6\rangle\,. \tag{42}$$

Therefore, the operator has eigenvalues ± 1 and is an integral of motion.
The commutator of $\hat{S}$ and $\hat{P}$ is

$$\hat{P}\hat{S} = (-1)^N \hat{S}\hat{P} \rightarrow [\hat{S}, \hat{P}] = \begin{cases} 0 & N \text{ even} \\ 2\hat{S}\hat{P} & N \text{ odd} \end{cases} \tag{43}$$

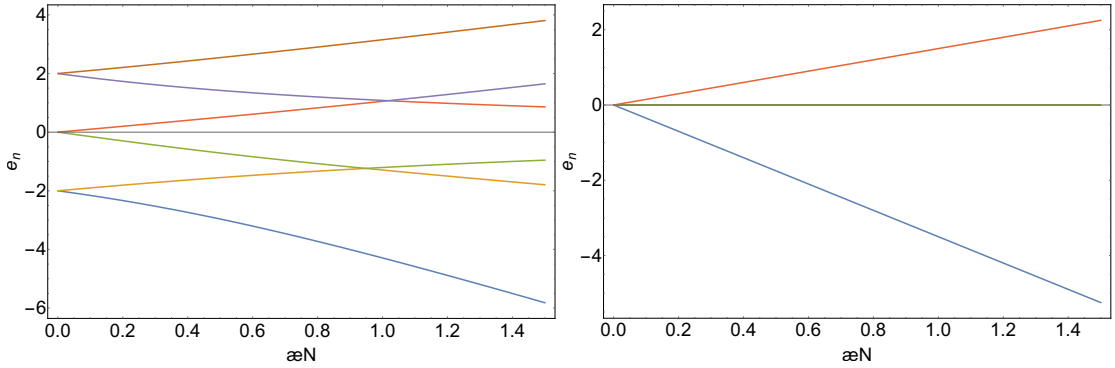

Figure 24: Plot of all eigenvalues of H_- with eigenvalue 1 of $\hat{S}$ on the left and -1 on the right.
$(N = 4, L = 0, E[\hat{S}] = \pm 1, E[\hat{P}] = -1)$

and hence only for an even number of particles we can be simultaneously in an eigenbasis of $\hat{S}$ and $\hat{P}$.
This enables us to revisit the crossing in figure (23) and split the spectrum in two, with eigenvalue ± 1 of the operator $\hat{S}$.
In figure (24) we can see that even though this crossing disappears two other crossings remain and both their gaps get closer than 10^{-15}, consequently there are still some unused integrals of motion left.
Checking crossings of other combinations of $N \in 2\mathbb{N}, L = 0, E[\hat{S}] = \pm 1$ and $E[\hat{P}] = \pm 1$ reveals that most (all) crossings, but the earlier two, are now avoided crossings.
Here $E[\hat{S}]$ is used equivalently to "eigenvalue of $\hat{S}$".
For an odd number of particles choosing a fixed eigenvalue of $\hat{S}$ results in the same degeneracy breaking we have already seen in figure (20).
This means that choosing the eigenvalue ± 1 of either $\hat{P}$ or $\hat{S}$ results in the same energies for an odd number of particles.

5.7. Approximation of the energies of the five-site-case via the three-site-case

The Hamiltonian in equation (13) is scale-invariant

$$\begin{aligned} H(x \to x' = ax) &= \frac{-i\hbar}{2ma} \sum_{\alpha=1}^{N} \frac{\partial}{\partial x_\alpha} \sigma_x^{(\alpha)} - 2R\alpha \sum_{\alpha \neq \beta, \alpha < \beta} \frac{1}{a} \delta(x_\alpha - x_\beta)(\sigma_z^\alpha \otimes \sigma_z^\beta) \\ &= \frac{1}{a} H(x). \end{aligned}$$

As a result, the eigenenergies of such a scaled system are simply connected through this factor to the eigenenergies of the unscaled system.
We can use this knowledge to approximate the eigenenergies of the five-site-case with

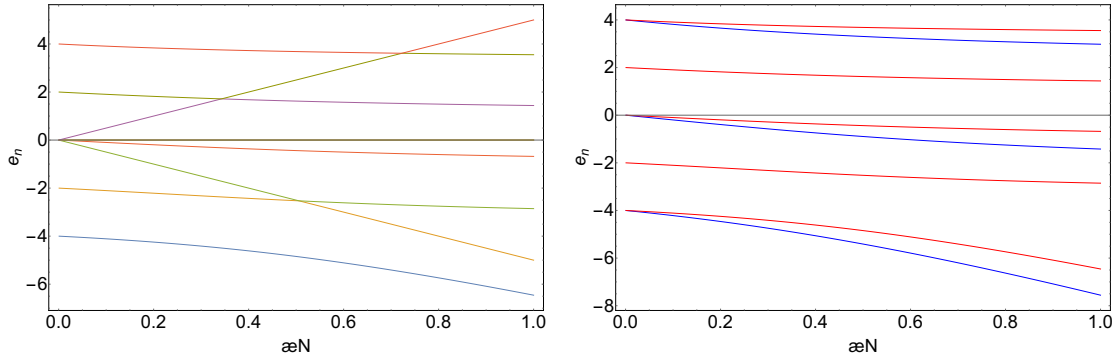

Figure 25: Full spectrum plot of the five-site-case for $N = 2, L = 0$ on the left. The right figure is a comparison of the energies of the rescaled three-site-case (blue) to the five-site-case (red) for $N = 2, L = 0, E[\hat{P}] = 1$.

the three-site-case. Using the definition of plane waves from equation (4), we get

$$\Psi_k(x \to x' = ax) = \frac{1}{\sqrt{R}} e^{i\frac{2\pi}{R}kax} = \Psi_{k'=ka}(x). \tag{44}$$

Thus adding higher k-modes is equivalent to adding them between the zeroth and first k-mode and then rescaling the whole system. The right figure of figure (25) is an energy plot of the exact five-site-case and an approximation through the three-site-case for states with eigenvalue one of the time-reverse operator. Unfortunately, it's not a good approximation of any energies as αN increases.

5.8. Solution of the n-site-case with the three-site-case for $N = 2, L = 0$

The always present approximation throughout this whole thesis is some form of truncation, i.e., cutting off all the k-modes higher than some threshold value $k_{\max}$ (and lower than $-k_{\max}$). This means, in the continuous case, where $k_{\max} \to \infty$, we no longer approximate.
While actually reaching indefinitely high modes is impossible, going to (relatively) high modes certainly isn't for some N, L.
From equation (21) we get for $N = 2, L = 0$ the following allowed states in the three-site-case

$$|0,2,0,0,0,0\rangle, |0,1,0,0,1,0\rangle, |0,0,0,0,2,0\rangle,$$
$$|1,0,1,0,0,0\rangle, |1,0,0,0,0,1\rangle, |0,0,1,1,0,0\rangle, |0,0,0,1,0,1\rangle$$

and in the five-site-case

$$|0,0,2,0,0,0,0,0,0,0\rangle\,,|0,0,1,0,0,0,0,1,0,0\rangle\,,|0,0,0,0,0,0,0,2,0,0\rangle\,,$$
$$|0,1,0,1,0,0,0,0,0,0\rangle\,,|0,1,0,0,0,0,0,0,1,0\rangle\,,|0,0,0,1,0,0,1,0,0,0\rangle\,,$$
$$|0,0,0,0,0,0,1,0,1,0\rangle\,,$$
$$|1,0,0,0,1,0,0,0,0,0\rangle\,,|1,0,0,0,0,0,0,0,0,1\rangle\,,|0,0,0,0,1,1,0,0,0,0\rangle\,,$$
$$|0,0,0,0,0,1,0,0,0,1\rangle \text{ with } |n_{2+},n_{1+},n_{0+},n_{-1+},n_{-2+},n_{2-},n_{1-},n_{0-},n_{-1-},n_{-2-}\rangle\,.$$

As we can see the first seven states of the five-site-case are the seven states of the three-site-case and using this recursive relation yields a repeating structure of the Hamiltonian matrix for the five-site-case:

$$H = H_0 - \alpha V = \begin{pmatrix}
0 & 0 & 0 & 0 & 0 & 0 & 0 & 0 & 0 & 0 & 0 \\
0 & 0 & 0 & 0 & 0 & 0 & 0 & 0 & 0 & 0 & 0 \\
0 & 0 & 0 & 0 & 0 & 0 & 0 & 0 & 0 & 0 & 0 \\
0 & 0 & 0 & 0 & 0 & 0 & 0 & 0 & 0 & 0 & 0 \\
0 & 0 & 0 & 0 & 2 & 0 & 0 & 0 & 0 & 0 & 0 \\
0 & 0 & 0 & 0 & 0 & -2 & 0 & 0 & 0 & 0 & 0 \\
0 & 0 & 0 & 0 & 0 & 0 & 0 & 0 & 0 & 0 & 0 \\
0 & 0 & 0 & 0 & 0 & 0 & 0 & 0 & 0 & 0 & 0 \\
0 & 0 & 0 & 0 & 0 & 0 & 0 & 0 & 4 & 0 & 0 \\
0 & 0 & 0 & 0 & 0 & 0 & 0 & 0 & 0 & -4 & 0 \\
0 & 0 & 0 & 0 & 0 & 0 & 0 & 0 & 0 & 0 & 0
\end{pmatrix}$$

three-site-case

$$-\alpha \begin{pmatrix}
0 & 0 & 2 & 0 & 0 & 0 & 2\sqrt{2} & 0 & 0 & 0 & 2\sqrt{2} \\
0 & 2 & 0 & 0 & 2 & 2 & 0 & 0 & 2 & 2 & 0 \\
2 & 0 & 0 & 2\sqrt{2} & 0 & 0 & 0 & 2\sqrt{2} & 0 & 0 & 0 \\
0 & 0 & 2\sqrt{2} & 0 & 0 & 0 & 4 & 0 & 0 & 0 & 4 \\
0 & 2 & 0 & 0 & 2 & 2 & 0 & 0 & 2 & 2 & 0 \\
0 & 2 & 0 & 0 & 2 & 2 & 0 & 0 & 2 & 2 & 0 \\
2\sqrt{2} & 0 & 0 & 4 & 0 & 0 & 0 & 4 & 0 & 0 & 0 \\
0 & 0 & 2\sqrt{2} & 0 & 0 & 0 & 4 & 0 & 0 & 0 & 4 \\
0 & 2 & 0 & 0 & 2 & 2 & 0 & 0 & 2 & 2 & 0 \\
0 & 2 & 0 & 0 & 2 & 2 & 0 & 0 & 2 & 2 & 0 \\
2\sqrt{2} & 0 & 0 & 4 & 0 & 0 & 0 & 4 & 0 & 0 & 0
\end{pmatrix}$$

If the matrix structure of the interaction part of the Hamiltonian of the five-site-case is,

$$V_{\text{five-site}} = \begin{pmatrix} \text{3x3} & \text{3x4} & \text{3x4} \\ \text{4x3} & \text{4x4} & \text{4x4} \\ \text{4x3} & \text{4x4} & \text{4x4} \end{pmatrix}$$

then the seven-site-case matrix is given by

$$V_{\text{seven-site}} = \begin{pmatrix} \text{3x3} & \text{3x4} & \text{3x4} & \text{3x4} \\ \text{4x3} & \text{4x4} & \text{4x4} & \text{4x4} \\ \text{4x3} & \text{4x4} & \text{4x4} & \text{4x4} \\ \text{4x3} & \text{4x4} & \text{4x4} & \text{4x4} \end{pmatrix}.$$

This enables us to plot the energies for $N = 2$ and $L = 0$ for different values of $k_{\max}$. In figures (26) we can see the 3-,11-,21-,101-,201-,1001-site-case respectively.
Only the groundstate and two exited energies strongly depend on the interaction, but the seemingly constant energies are not, as we can see in figure (28).
This energy behavior actually confirms my advisor's (Benjamin Geiger) prediction that the continuous case has the energies:

$$E_n(\alpha) = 2n + \frac{2}{\pi}\arctan(-\pi\alpha)$$

Furthermore, the slope of the linear increase of the two energies converges against $\pm k_{\max}$. Therefore, these two energies are only present in the truncated model since in the continuous case $k_{\max} = \infty$.
This also implies that for any $k_{\max}$ at $\alpha N = 1$ the two linear energies separate from the very dense energy spectrum.
We may recall that adding two sites results in four additional energies of the system - one at $k_{\max}$, one at $-k_{\max}$ and two at exactly zero energy. Thus, this interaction-independent energy zero is endlessly degenerate in the continuous case, and the density of states is a constant with a delta-function at zero energy.
The lower energy converges against the ground state energy for an increasing αN as we can see in figure (27).

5.9. Attractive and repulsive case due to spin swap symmetry

The energy spectrum of the attractive case ($\alpha < 0$) is identical to the inverted energy spectrum of the same system in the repulsive case ($\alpha > 0$). This means that we can reproduce the energy spectrum of the attractive case via the repulsive case and vice versa by simply inverting it - visible in figure (29).
To be more precise the operator defined by

$$\hat{S}\,|\sigma\rangle = |\gamma\rangle \;\text{ with } \sigma \neq \gamma \tag{45}$$

inverts all spin values and it acting on the Hamiltonian given in equation (17) delivers:

$$\begin{aligned} \hat{S}H(\alpha)\hat{S}^\dagger &= \hat{S}\left(H_0 - \alpha\left(\underbrace{H_{diag} + H_{offdiag} + H_{offdiag}^\dagger}_{=H_1}\right)\right)\hat{S}^\dagger \\ &= \underbrace{-H_0 - \alpha H_1}_{\text{same eigenvalues as } H(\alpha) = H_0 - \alpha H_1} = -\left(H_0 + \alpha H_1\right) = -H(-\alpha) \end{aligned} \tag{46}$$

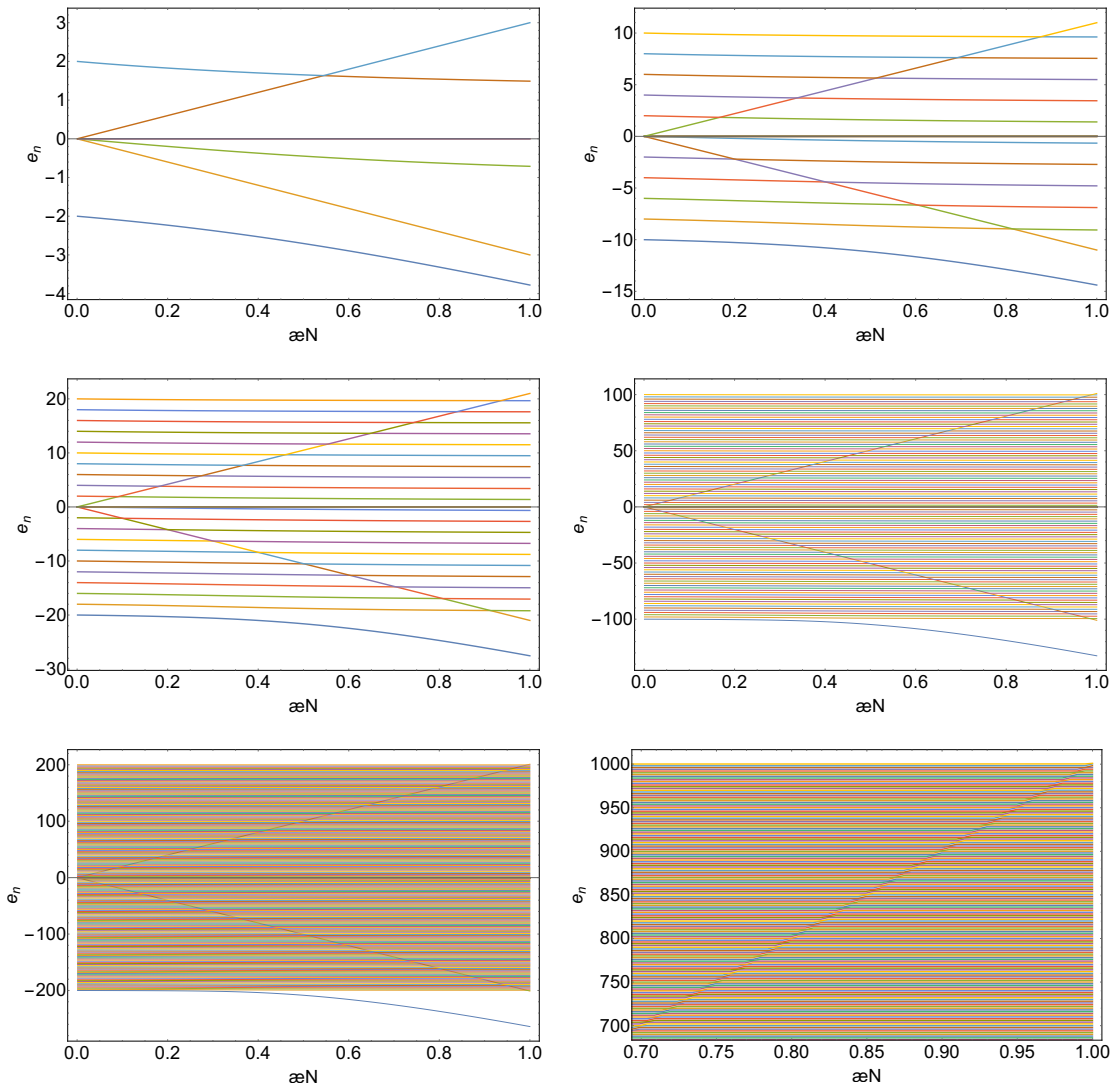

Figure 26: Full spectrum plot for fixed $N = 2$ and $L = 0$ and different $k_{\max} = \{1, 5, 10, 50, 100, 500\}$ values - from top left to bottom right. Allowing high k-modes results in only three energies depending on the interaction, the ground-state and two exited energies. The two exited energies rise linearly.

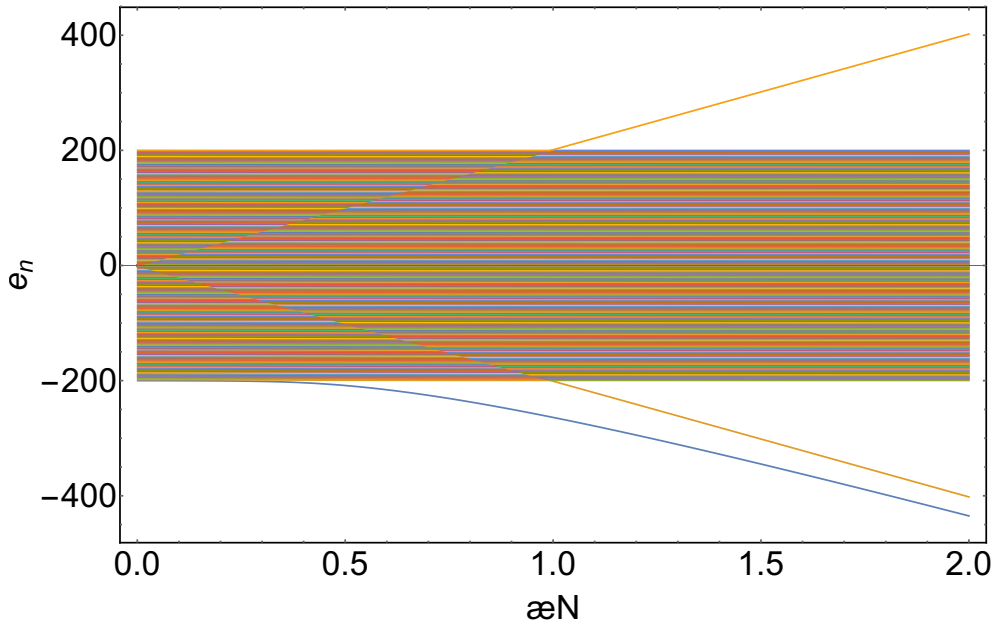

Figure 27: Full spectrum plot for $N = 2, L = 0, k_{\max} = 100$ - the two linearly rising energies separate from the dense energy spectrum at a constant $\alpha N = 1$.

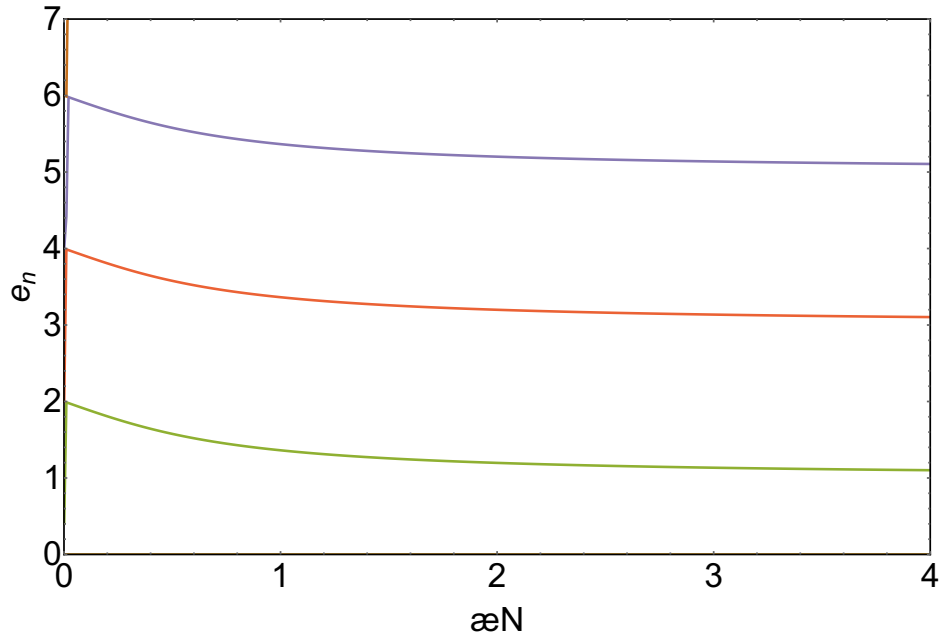

Figure 28: Cutout of the energy plot for $N = 2, L = 0$ and $k_{\max} = 200$. The seemingly interaction-independent energies aren't interaction-independent.

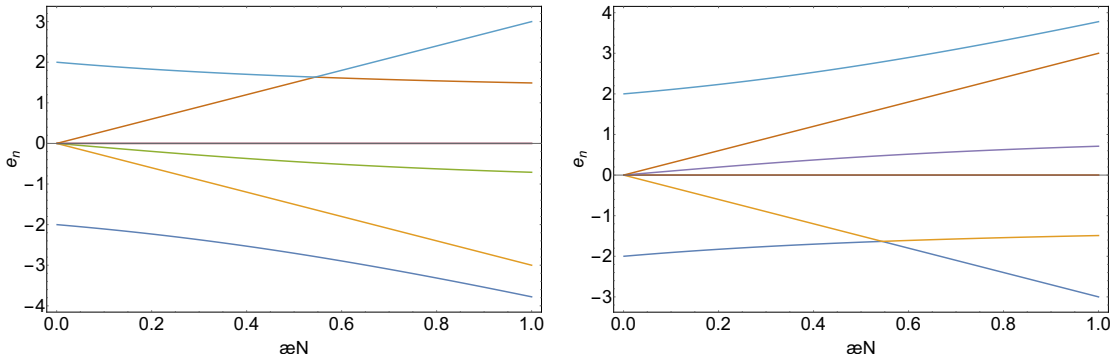

Figure 29: Full spectrum plot of the attractive case on the left and repulsive case on the right for $N = 2, L = 0, n_{max} = 7$.

5.10. Thermodynamics of the system

We assume a canonical ensemble, i.e., the system defined by the Hamiltonian (17) is in thermal contact with a much bigger reservoir with a constant temperature T. The system itself can be very small (even 2 particles). The reservoir does not change due to the contact with the system and is only allowed to exchange energy while keeping the total energy constant. Consequently, the total system is isolated[4].
The thermodynamic potential of the canonical ensemble is the (Helmholz) free energy

$$F(T, V, N) = -k_b T \ln(Z) \tag{47}$$

with the partition sum

$$Z = \sum_n e^{-\frac{E_n}{k_b T}}. \tag{48}$$

5.10.1. Heat capacity

The internal energy and heat capacity are then easily calculable with

$$\bar{E} = \sum_n p_n E_n = -\frac{\partial \ln(Z)}{\partial \beta} \text{ with } \beta = \frac{1}{k_b T}, \tag{49}$$

$$C_v = \left(\frac{\partial \bar{E}}{\partial T}\right)_V. \tag{50}$$

We set Boltzmann's constant to one ($k_b = 1$) and plot the heat capacity for $N = 4$ in figure (30) and $N = 10$ in figure (31). In both cases the total momentum L vanishes ($L = 0$).
We see that with an increasing coupling constant the maximum value of the heat capacity shifts away from temperature one to higher temperatures.

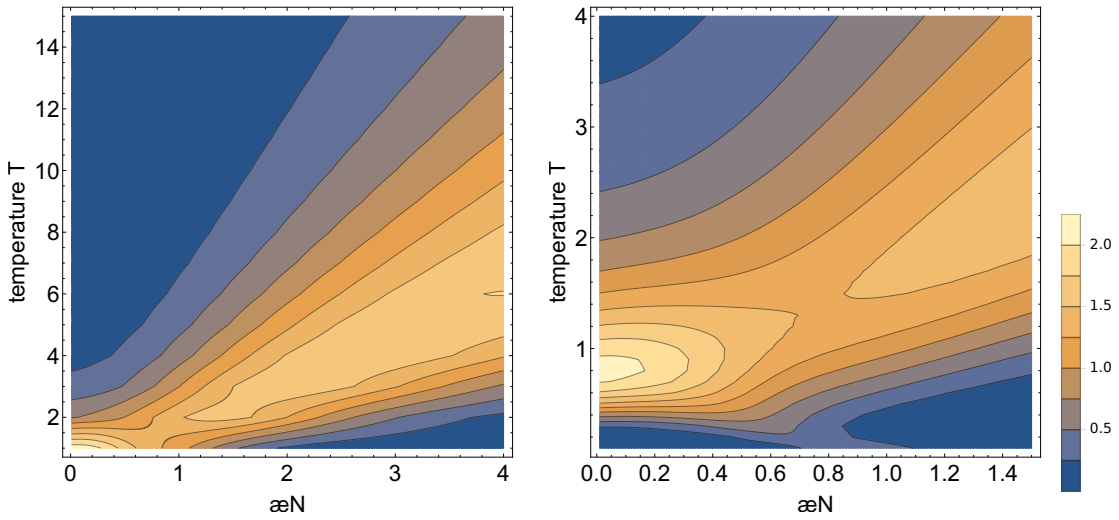

Figure 30: Heat capacity as a function of T and αN for $N = 4$ particles. The maximum shifts to higher temperatures for increasing αN.

5.10.2. Chemical potential

The chemical potential is defined as

$$\mu = \left(\frac{\partial F}{\partial N}\right)_{T,V}. \tag{51}$$

As the derivative of the free energy with respect to N is only plausible in the thermal limit, one can alternatively look at the quantity

$$M(N) = \frac{F(N+1) - F(N)}{N+1-N} = F(N+1) - F(N) \tag{52}$$

and plot the free energy and "chemical potential" while varying the number of particles and keeping either the temperature or the combined parameter αN fixed. In both instances the total momentum is equal to zero.
These plots are seen in figures (32) and (33). The chemical potential is strictly lower for an odd number of particles.

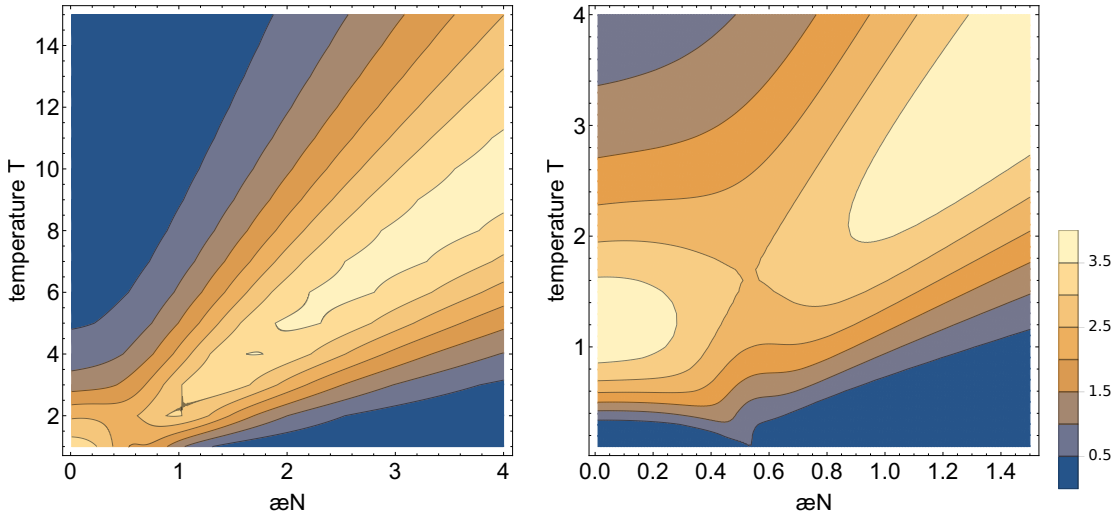

Figure 31: Heat capacity as a function of T and αN for $N = 10$ particles. The maximum shifts to higher temperatures for increasing αN.

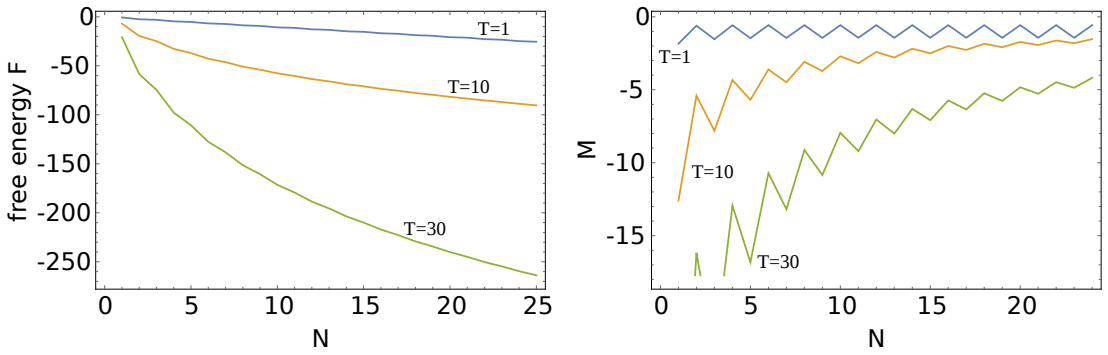

Figure 32: F and M as a function of the number of particles. $\alpha N = 0.01$ is constant. For $T = 1$ the "chemical potential" M converges against two different values for an even and odd number of particles, respectively.

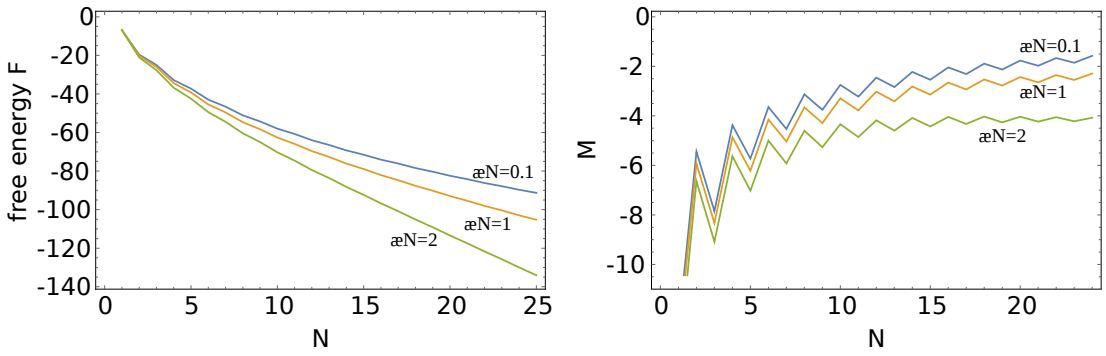

Figure 33: F and M as a function of the number of particles. $T = 10$ is constant. The "chemical potential" M is strictly lower for an odd number of particles. This gap closes as the number of particles increases.

6. Conclusion

The Truncated Lieb-Liniger model has some fascinating properties. Even in its simplest incarnation, with just three allowed k-modes, it already shows phenomena like an energy gap narrowing around the critical point and a converging shift of this critical point towards $\alpha N = 1$ with an increasing number of particles.
While the five-site-case with parabolic dispersion relation doesn't have any more crossing eigenenergies, the five-site-case with linear dispersion relation does. Thus, fixing the number of particles and total momentum of the system keeps all integrals of motion only in the parabolic case constant.
In the linear case of the five-site model the position of the excitation energy minimum shifts to one $\propto N^{-1.5}$ and the energy of the excitation energy minimum converges to zero $\propto \frac{1}{\sqrt{N}}$. These values differ from the ones obtained for the five-site-case with parabolic dispersion relation.
Lastly, we use this modeling to approximate the behavior of a bosonic system with a two band structure in the environment of a crossing in its dispersion relation. We find two more integrals of motion, the time-reverse operator and a spin-parity-operator, which enable us to (almost) completely eliminate all crossings.
Furthermore, we can confirm Kramers-Theorem and the degeneracy breaking due to a magnetic field and are able to reproduce the repulsive case via the attractive case by inverting the energy spectrum and vice versa.
Moreover, the system's Hamiltonian is scale-invariance and we can use this invariance to approximate energies of higher site-cases by solving the three-site-case and rescaling it - it turns out to be a rather poor approximation for all energies as αN increases.
Finally, we have seen that solving the three-site-case is enough to exactly solve any higher site-case or rather compute its Hamiltonian matrix, at least for some combinations of N, L. This procedure is exemplary shown for $N = 2, L = 0$, and we obtain that all energies but three are almost interaction-independent and that the density of states peaks at zero energy.
Interesting results can also be found in the thermodynamics of the system. The maximum of the heat capacity shifts to higher temperatures for an increasing αN, and the chemical potential converges to two different values as the number of particles increases depending on whether the number of particles of the system is even or odd.
Regarding a continuation of this topic - there are two obvious starting points. $N, L, \hat{P}$ and $\hat{S}$ seem to not be the only integrals of motion since fixing them did not eliminate all crossings as we saw in section 5.6.1 - what else is preserved ?
The second approach could be to allow even higher k-modes. The problem will quickly become to write very efficient code since the dimension of the Hamiltonian matrix will rise drastically.

A. Appendix

$$
\begin{aligned}
H &= a^\dagger_{1+}a_{1+} - a^\dagger_{1-}a_{1-} - a^\dagger_{-1+}a_{-1+} + a^\dagger_{-1-}a_{-1-} - \alpha\Big[\\
&\quad \sum_{\substack{k,l,m,n=\pm1,0 \\ \sigma\neq\gamma}} \delta_{k+l,m+n}\left(a^\dagger_{k\sigma}a^\dagger_{l\sigma}a_{m\gamma}a_{n\gamma} + a^\dagger_{k\sigma}a^\dagger_{l\gamma}a_{m\sigma}a_{n\gamma}\right)\Big] \\
&= a^\dagger_{1+}a_{1+} - a^\dagger_{1-}a_{1-} - a^\dagger_{-1+}a_{-1+} + a^\dagger_{-1-}a_{-1-} - \alpha\Big[\\
&\quad \sum_{\substack{k,l,m,n=\pm1,0 \\ k=m,l=n \\ \sigma\neq\gamma}} \left(a^\dagger_{k\sigma}a^\dagger_{l\sigma}a_{m\gamma}a_{n\gamma} + a^\dagger_{k\sigma}a^\dagger_{l\gamma}a_{m\sigma}a_{n\gamma}\right) + \\
&\quad \sum_{\substack{k,l,m,n=\pm1,0 \\ k\neq m,l\neq n \\ \sigma\neq\gamma}} \delta_{k+l,m+n}\left(a^\dagger_{k\sigma}a^\dagger_{l\sigma}a_{m\gamma}a_{n\gamma} + a^\dagger_{k\sigma}a^\dagger_{l\gamma}a_{m\sigma}a_{n\gamma}\right)\Big] \\
&= a^\dagger_{1+}a_{1+} - a^\dagger_{1-}a_{1-} - a^\dagger_{-1+}a_{-1+} + a^\dagger_{-1-}a_{-1-} - \alpha\Big[\\
&\quad \sum_{\substack{k,l,m,n=\pm1,0 \\ k=m,l=n \\ k\neq l \\ \sigma\neq\gamma}} \left(a^\dagger_{k\sigma}a^\dagger_{l\sigma}a_{m\gamma}a_{n\gamma} + a^\dagger_{k\sigma}a^\dagger_{l\gamma}a_{m\sigma}a_{n\gamma}\right) + \\
&\quad \sum_{\substack{k,l,m,n=\pm1,0 \\ k=m,l=n \\ k=l \\ \sigma\neq\gamma}} \left(a^\dagger_{k\sigma}a^\dagger_{l\sigma}a_{m\gamma}a_{n\gamma} + a^\dagger_{k\sigma}a^\dagger_{l\gamma}a_{m\sigma}a_{n\gamma}\right) + \\
&\quad \sum_{\substack{k,l,m,n=\pm1,0 \\ k\neq m,l\neq n \\ k=n,l=m \\ \sigma\neq\gamma}} \left(a^\dagger_{k\sigma}a^\dagger_{l\sigma}a_{m\gamma}a_{n\gamma} + a^\dagger_{k\sigma}a^\dagger_{l\gamma}a_{m\sigma}a_{n\gamma}\right) + \\
&\quad \sum_{\substack{k,l,m,n=\pm1,0 \\ k\neq m,l\neq n \\ k\neq n,l\neq m \\ \sigma\neq\gamma}} \delta_{k+l,m+n}\left(a^\dagger_{k\sigma}a^\dagger_{l\sigma}a_{m\gamma}a_{n\gamma} + a^\dagger_{k\sigma}a^\dagger_{l\gamma}a_{m\sigma}a_{n\gamma}\right)\Big] \\
&= a^\dagger_{1+}a_{1+} - a^\dagger_{1-}a_{1-} - a^\dagger_{-1+}a_{-1+} + a^\dagger_{-1-}a_{-1-} - \alpha\Big[\\
&\quad \sum_{\substack{k,l=\pm1,0 \\ k<l \\ \sigma\neq\gamma}} 2\left(a^\dagger_{k\sigma}a^\dagger_{l\sigma}a_{k\gamma}a_{l\gamma} + a^\dagger_{k\sigma}a^\dagger_{l\gamma}a_{k\sigma}a_{l\gamma}\right) +
\end{aligned}
$$

$$\sum_{\substack{k=\pm1,0\\ \sigma\neq\gamma}} \left(a^\dagger_{k\sigma}a^\dagger_{k\sigma}a_{k\gamma}a_{k\gamma} + a^\dagger_{k\sigma}a^\dagger_{k\gamma}a_{k\sigma}a_{k\gamma}\right) +$$

$$\sum_{\substack{k,l=\pm1,0\\ k<l\\ \sigma\neq\gamma}} 2\left(a^\dagger_{k\sigma}a^\dagger_{l\sigma}a_{l\gamma}a_{k\gamma} + a^\dagger_{k\sigma}a^\dagger_{l\gamma}a_{l\sigma}a_{k\gamma}\right) +$$

$$\sum_{\substack{k,l,m,n=\pm1,0\\ k\neq m,l\neq n\\ k\neq n,l\neq m\\ \sigma\neq\gamma}} \delta_{k+l,m+n}\left(a^\dagger_{k\sigma}a^\dagger_{l\sigma}a_{m\gamma}a_{n\gamma} + a^\dagger_{k\sigma}a^\dagger_{l\gamma}a_{m\sigma}a_{n\gamma}\right)\Big]$$

$$= a^\dagger_{1+}a_{1+} - a^\dagger_{1-}a_{1-} - a^\dagger_{-1+}a_{-1+} + a^\dagger_{-1-}a_{-1-} - \alpha\Big[$$

$$\sum_{\substack{k,l=\pm1,0\\ k<l\\ \sigma\neq\gamma}} 4a^\dagger_{k\sigma}a^\dagger_{l\sigma}a_{k\gamma}a_{l\gamma} +$$

$$\sum_{\substack{k=\pm1,0\\ \sigma\neq\gamma}} \left(a^\dagger_{k\sigma}a^\dagger_{k\sigma}a_{k\gamma}a_{k\gamma} + a^\dagger_{k\sigma}a^\dagger_{k\gamma}a_{k\sigma}a_{k\gamma}\right) +$$

$$\sum_{\substack{k,l=\pm1,0\\ k<l\\ \sigma\neq\gamma}} 2\left(a^\dagger_{k\sigma}a^\dagger_{l\gamma}a_{k\sigma}a_{l\gamma} + a^\dagger_{k\sigma}a^\dagger_{l\gamma}a_{l\sigma}a_{k\gamma}\right) +$$

$$\sum_{\substack{k,l,m,n=\pm1,0\\ k\neq m,l\neq n\\ k\neq n,l\neq m\\ \sigma\neq\gamma}} \delta_{k+l,m+n}\left(a^\dagger_{k\sigma}a^\dagger_{l\sigma}a_{m\gamma}a_{n\gamma} + a^\dagger_{k\sigma}a^\dagger_{l\gamma}a_{m\sigma}a_{n\gamma}\right)\Big]$$

$$= n_{1+} - n_{1-} - n_{-1+} + n_{-1-} - \alpha\Big[$$

$$\sum_{\substack{k,l=\pm1,0\\ k<l}} 4\left(a^\dagger_{k+}a^\dagger_{l+}a_{k-}a_{l-} + (a^\dagger_{k+}a^\dagger_{l+}a_{k-}a_{l-})^\dagger\right)$$

$$\sum_{k=\pm1,0} \left(a^\dagger_{k+}a^\dagger_{k+}a_{k-}a_{k-} + (a^\dagger_{k+}a^\dagger_{k+}a_{k-}a_{k-})^\dagger + 2n_{k+}n_{k-}\right) +$$

$$\sum_{\substack{k,l=\pm1,0\\ k<l}} 2\left(n_{k+}n_{l-} + n_{k-}n_{l+} + a^\dagger_{k+}a^\dagger_{l-}a_{l+}a_{k-} + (a^\dagger_{k+}a^\dagger_{l-}a_{l+}a_{k-})^\dagger\right) +$$

$$\sum_{\sigma\neq\gamma} 2\left(a^\dagger_{1\sigma}a^\dagger_{-1\sigma}a_{0\gamma}a_{0\gamma} + a^\dagger_{1\sigma}a^\dagger_{-1\gamma}a_{0\sigma}a_{0\gamma} + \left(a^\dagger_{1\sigma}a^\dagger_{-1\sigma}a_{0\gamma}a_{0\gamma} + a^\dagger_{1\sigma}a^\dagger_{-1\gamma}a_{0\sigma}a_{0\gamma}\right)^\dagger\right)\Big]$$

$$= H_0 - \alpha\left(H_{diag} + H_{offdiag} + H^\dagger_{offdiag}\right)$$

with

$$H_0 = n_{1+} - n_{1-} - n_{-1+} + n_{-1-}$$

$$H_{diag} = 2 \sum_{k=\pm1,0} \left[n_{k+} n_{k-} + \sum_{\substack{l=\pm1,0 \\ l>k}} (n_{k+} n_{l-} + n_{k-} n_{l+}) \right]$$

$$H_{offdiag} = \sum_{\substack{k,l=\pm1,0 \\ k<l}} \left(4 a^\dagger_{k+} a^\dagger_{l+} a_{k-} a_{l-} + 2 a^\dagger_{k+} a^\dagger_{l-} a_{l+} a_{k-} \right) + \sum_{k=\pm1,0} a^\dagger_{k+} a^\dagger_{k+} a_{k-} a_{k-} + \sum_{\sigma \neq \gamma} 2 \left(a^\dagger_{1\sigma} a^\dagger_{-1\sigma} a_{0\gamma} a_{0\gamma} + a^\dagger_{1\sigma} a^\dagger_{-1\gamma} a_{0\sigma} a_{0\gamma} \right)$$

List of Figures

References

[1] Quantenmechanik für Fortgeschrittene (QM 2) by Franz Schwabl
Springer, Berlin Heidelberg , Fifth Edition
ISBN 13: 978-3-540-85075-5; DOI 10.1007/978-3-540-85076-2
Springer-Lehrbuch ISSN 0937-7433

[2] Mathematica-Sheet "Exact-Diagonalization.nb" by Benjamin Geiger

[3] Quantenmechanik. Band 2 by Albert Messiah
Walter de Gruyter, Berlin, Second Edition
ISBN 10: 3-11-010265-X, ISBN 13: 978-3-110-10265-9

[4] Lecture notes on "Quantum statistics" held by Prof. Dr. Jaroslav Fabian
Written in LaTeX by Florian Rappl, 07/20/2010

[5] Modern Quantum Mechanics by J.J. Sakurai and Jim Napolitano
Publisher Pearson, New York City, Second Edition
ISBN 10: 0-321-50336-8; ISBN 13: 978-0-321-50336-7

[6] Exact Analysis of an Interacting Bose Gas. 1.The General Solution and the Ground State by Elliot H. Lieb and Werner Liniger
Phys. Rev. 130, 1605 (1963)

[7] Algebraic Aspects of Bethe-Ansatz by L.D. Faddeev
Lectures delivered by L.D. Faddeev at the Institute for Theoretical Physics at Stony Brook university, written by Kostas Skenderis
DOI: 10.1142/S0217751X95000905 Cite as: arXiv:hep-th/9404013

[8] The Ehrenfest Classification of Phase Transitions: Introduction and Evolution by G. Jaeger
Springer, Berlin Heidelberg 1998
DOI: 10.1007/s004070050021, Arch Hist Exact Sc. (1998) Volume 53

[9] Quantum phase transition in one-dimensional Bose-Einstein condensates with attractive interactions by Rina Kanamoto, Hiroki Saito, and Masahito Ueda
Phys. Rev. A 67, 013608 - Published 23 January 2003
DOI: https://doi.org/10.1103/PhysRevA.67.013608

[10] Black holes and quantumness on macroscopic scales by Daniel Flassig, Alexander Pritzel, and Nico Wintergerst
Phys. Rev. D 87, 084007 - Published 2 April 2013
DOI: https://doi.org/10.1103/PhysRevD.87.084007

[11] Semiclassical Theory of Few- and Many-body Quantum Systems with Short-range Interactions by Dr. Q. Hummel
PhD thesis of the University of Regensburg, 2018
URN: urn:nbn:de:bvb:355-epub-364236

An dieser Stelle möchte ich mich gerne bei all denjenigen bedanken, die mich bei dem Erstellen dieser Bachelorarbeit unterstützt haben.

Zuerst gilt mein Dank Prof. Dr. Klaus Richter, der mir diese Bachelorarbeit in seinem Lehrstuhl ermöglicht und betreut hat.

Ebenfalls gebührt mein Dank Herr Benjamin Geiger, der mich mit viel Geduld und Hilfsbereitschaft unterstützt hat.

Außerdem bedanke ich mich bei dem gesamten Lehrstuhl für die herzliche Aufnahme und gute Atmosphäre.

Abschließend möchte ich mich bei meinen Eltern bedanken, die mir mein Studium durch ihre Unterstützung ermöglicht haben.

Simon Bachhuber,
Regensburg

Ich habe die Arbeit selbstständig verfasst, keine anderen als die angegebenen Quellen und Hilfsmittel benutzt und bisher keiner anderen Prüfungsbehörde vorgelegt. Außerdem bestätige ich hiermit, dass die vorgelegten Druckexemplare und die vorgelegte elektronische Version der Arbeit identisch sind, dass ich über wissenschaftlich korrektes Arbeiten und Zitieren aufgeklärt wurde und dass ich von den in §24 Abs. 5 vorgesehenen Rechtsfolgen Kenntnis habe.

Regensburg